

University of Montana

ScholarWorks at University of Montana

Graduate Student Theses, Dissertations, &
Professional Papers

Graduate School

1999

Identification and characterization of inhibitors of L-glutamate transport into rat brain synaptic vesicles

Richard D. Bartlett
The University of Montana

Follow this and additional works at: <https://scholarworks.umt.edu/etd>

Let us know how access to this document benefits you.

Recommended Citation

Bartlett, Richard D., "Identification and characterization of inhibitors of L-glutamate transport into rat brain synaptic vesicles" (1999). *Graduate Student Theses, Dissertations, & Professional Papers*. 10554.
<https://scholarworks.umt.edu/etd/10554>

This Dissertation is brought to you for free and open access by the Graduate School at ScholarWorks at University of Montana. It has been accepted for inclusion in Graduate Student Theses, Dissertations, & Professional Papers by an authorized administrator of ScholarWorks at University of Montana. For more information, please contact scholarworks@mso.umt.edu.

INFORMATION TO USERS

This manuscript has been reproduced from the microfilm master. UMI films the text directly from the original or copy submitted. Thus, some thesis and dissertation copies are in typewriter face, while others may be from any type of computer printer.

The quality of this reproduction is dependent upon the quality of the copy submitted. Broken or indistinct print, colored or poor quality illustrations and photographs, print bleedthrough, substandard margins, and improper alignment can adversely affect reproduction.

In the unlikely event that the author did not send UMI a complete manuscript and there are missing pages, these will be noted. Also, if unauthorized copyright material had to be removed, a note will indicate the deletion.

Oversize materials (e.g., maps, drawings, charts) are reproduced by sectioning the original, beginning at the upper left-hand corner and continuing from left to right in equal sections with small overlaps. Each original is also photographed in one exposure and is included in reduced form at the back of the book.

Photographs included in the original manuscript have been reproduced xerographically in this copy. Higher quality 6" x 9" black and white photographic prints are available for any photographs or illustrations appearing in this copy for an additional charge. Contact UMI directly to order.

UMI

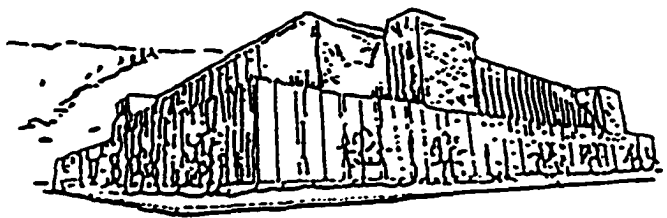
A Bell & Howell Information Company
300 North Zeeb Road, Ann Arbor MI 48106-1346 USA
313/761-4700 800/521-0600

NOTE TO USERS

The original manuscript received by UMI contains pages with light print. Pages were microfilmed as received.

This reproduction is the best copy available

UMI



Maureen and Mike
MANSFIELD LIBRARY

The University of **MONTANA**

Permission is granted by the author to reproduce this material in its entirety, provided that this material is used for scholarly purposes and is properly cited in published works and reports.

*** Please check "Yes" or "No" and provide signature ***

Yes, I grant permission X
No, I do not grant permission

Author's Signature Richard D. Bartlett

Date 2/6/99

Any copying for commercial purposes or financial gain may be undertaken only with the author's explicit consent.

**IDENTIFICATION AND CHARACTERIZATION OF INHIBITORS
OF L-GLUTAMATE TRANSPORT INTO RAT BRAIN
SYNAPTIC VESICLES**

by

Richard D. Bartlett

B.S. Texas A&M at Corpus Christi, 1989

Presented in partial fulfillment of the requirements

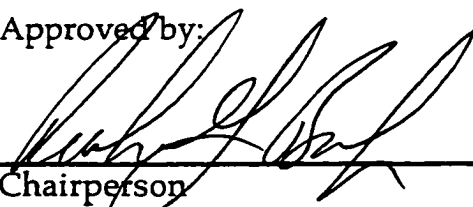
for the degree of Doctor of Philosophy

Department of Pharmaceutical Sciences

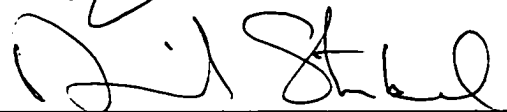
The University of Montana

1999

Approved by:



Chairperson



Dean, Graduate School

2-10-99

Date

UMI Number: 9918542

**UMI Microform 9918542
Copyright 1999, by UMI Company. All rights reserved.**

**This microform edition is protected against unauthorized
copying under Title 17, United States Code.**

UMI
300 North Zeeb Road
Ann Arbor, MI 48103

Identification and characterization of inhibitors of L-glutamate transport into rat brain synaptic vesicles (96 pp.)

Research advisor: Richard J. Bridges, Ph.D. 

The accumulation of L-glutamate into synaptic vesicles represents a key component of excitatory amino acid (EAA) transmission. It functions to divert glutamate from its normal metabolic activities and towards its role as a neurotransmitter. Vesicular glutamate uptake is achieved by a specific transport protein located in the membranes of synaptic vesicles which is remarkably selective for L-glutamate. Uptake is driven by an electrochemical proton gradient generated by a vacuolar-type proton ATPase and is characterized by a low affinity for L-glutamate ($K_m = 1-3$ mM). In this study, two classes of competitive inhibitors are presented which potently attenuate glutamate uptake via this transport system. These compounds are based upon rigid bicyclic molecular frameworks of quinoline and naphthylamine. Of the quinolines, two analogues of kynurenate (xanthurenate and 7-Cl-kynurenate) which contain electron donating groups attached to the carbocyclic ring were found to be more potent inhibitors than kynurenate itself. Using molecular modeling studies, it is demonstrated that the carbocyclic quinoline ring may approximate the distal carboxylate of L-glutamate, and this correspondence is enhanced by these electron donating groups. Of the naphthylamines, several heterocyclic organic dyes were identified which inhibited vesicular glutamate uptake at nanomolar concentrations. These include Evans Blue, Chicago Sky Blue, Naphthol Blue Black, and Congo Red. Curiously, a direct structural comparison of these compounds to L-glutamate is difficult. Additionally it was found that appending diazo-linked aromatic side chains to the naphthylamine core dramatically increased inhibitory activity, suggesting that these compounds may bind to the vesicular transporter site in a fashion different than that of L-glutamate, perhaps via a lipophilic interaction.

Insight into the mechanism of vesicular glutamate transport was made by monitoring the efflux of accumulated ^3H -L-glutamate in the presence of these competitive inhibitors. It was observed that at concentrations ensuring saturation of the substrate binding site (i.e. $10\times$ the inhibitor K_i value), certain compounds stimulated efflux while others blocked it. Presumably, this efflux stimulation is due to homo- or hetero-exchange of the vesicular contents with an excellent substrate, while efflux attenuation is caused by compounds that are partial or non-substrate inhibitors. This approach provides a detailed pharmacological and mechanistic means to rapidly differentiate substrates from nonsubstrates at the vesicular glutamate transporter.

TABLE OF CONTENTS

Abstract.....	ii
List of tables.....	iv
List of figures.....	vi
Acknowledgments.....	viii
Chapter 1: Background and introduction.....	1
Chapter 2: Methods and materials.....	10
Chapter 3: Vesicular pharmacology of quinoline and pyridine based inhibitors.....	18
Chapter 4: Inhibition of vesicular glutamate uptake by naphthalene sulfonic acid dyes.....	35
Chapter 5: Characterization of the vesicular transporter mechanism: Roles of ATP-dependence, trans-stimulation, and efflux attenuation.....	57
Chapter 6: Cross-reactivities of EAA analogues with the vesicular glutamate transporter.....	80
Chapter 7: Conclusions and future directions.....	86

LIST OF TABLES

Table 3.1. Inhibitory activities of kynurenate analogues on the vesicular uptake of L-glutamate.....	20
Table 3.2. Kinetic analyses of kynurenic acid analogues as competitive inhibitors of ³ H-L-glutamate uptake into synaptic vesicles.....	24
Table 3.3. Activity of kynurenate analogs in inhibiting the uptake of ³ H-D-aspartate into synaptosomes isolated from rat forebrain.....	26
Table 3.4. Pharmacological specificity of kynurenic acid analogues as inhibitors of EAA ionotropic receptor binding.....	27
Table 4.1. Inhibition of ³ H-L-glutamate uptake into synaptic vesicles by naphthalene sulfonic acids.....	39
Table 4.2. Inhibition of ³ H-L-glutamate uptake into synaptic vesicles by naphthalene sulfonic acids.....	40
Table 4.3. Inhibitory potencies of naphthalene sulfonic acids on vesicular ³ H-L-glutamate uptake.....	42
Table 4.4. Inhibitory activities of naphthalene sulfonic acids on the uptake of ³ H-D-aspartate into rat forebrain synaptosomes.....	48

Table 4.5. Pharmacological specificity of naphthalene sulfonic acids as inhibitors of EAA ionotropic receptor binding.....	49
Table 6.1. Cross-reactivities of EAA analogues with the vesicular glutamate transporter.....	81

LIST OF FIGURES

Figure 1.1. Putative model of the bioenergetics of vesicular glutamate uptake.....	5
Figure 3.1. Demonstration of the competitive inhibition by xanthurenate on ³ H-L-glutamate uptake into synaptic vesicles.....	23
Figure 3.2. Depiction of the overlap of the distal carboxylates of L-glutamate and (1R,3S)-ACPD with the electron density above the carbocyclic ring of xanthurenate.....	31
Figure 3.3. Depiction of the overlap of the distal carboxylates of L-glutamate and (1R,3S)-ACPD with the electron density below the carbocyclic ring of xanthurenate.....	32
Figure 4.1. Demonstration of the inhibitory dose-response dependency of naphthalene sulfonic acids on ³ H-L-glutamate uptake into synaptic vesicles.....	41
Figure 4.2. Demonstration of the competitive inhibition by Congo Red on ³ H-L-glutamate uptake into synaptic vesicles.....	44
Figure 4.3. Demonstration of the competitive inhibition by Naphthol Blue Black on ³ H-L-glutamate uptake into synaptic vesicles.....	45

Figure 4.4. Depiction of glutamate, naphthylamine sulfonic acid dyes, and an overlay of both showing the potential vesicular glutamate binding conformation.....	54
Figure 5.1. ATP dependence of vesicular ³ H-L-glutamate accumulation and retention.....	62
Figure 5.2. Dependence of vesicular ³ H-L-glutamate retention on ATP.....	63
Figure 5.3. Time course for the ATP-dependent uptake of ³ H-L-glutamate into synaptic vesicles.....	65
Figure 5.4. Effect of temperature on ³ H-L-glutamate efflux from synaptic vesicles.....	67
Figure 5.5. Stimulatory effect of exogenous L-glutamate on the efflux of ³ H-L-glutamate from synaptic vesicles.....	68
Figure 5.6. Inhibitory effect of Congo Red on the efflux of ³ H-L-glutamate from synaptic vesicles.....	70
Figure 5.7. Inhibitory effects of vesicular glutamate transport inhibitors on the efflux of ³ H-L-glutamate from synaptic vesicles.....	71
Figure 5.8. Model of glutamate induced <i>trans</i> -stimulation for the vesicular transport system.....	75

ACKNOWLEDGMENTS

The completion of this research project would have been impossible, had it not been for the assistance of those who helped at various stages along the way. With sincere gratitude I wish to acknowledge that help, for the culmination of this study is as much a testimony to their efforts as that of my own. I would first and foremost like to thank my research advisor, Dr. Richard Bridges, for his guidance in experimental design and assistance in the preparation of this manuscript. It has been a pleasure and honor to work with you. Thanks to Dr. Charles Thompson, Dr. Keith Parker, Dr. Charles Eyer, and Dr. Barbara Wright for their insightful suggestions and assistance with the manuscript revisions. A special thanks to those who helped generate portions of the experimental data; Hans Koch, Danielle Dauenhauer, Jennifer Hensley, and Taren Grass. Thanks to Dr. Sean Esslinger for his assistance with the molecular modeling and guidance in the world of Chemistry. Thanks to Dr. Vernon Grund, the Dept. of Pharmaceutical Sciences, and the Graduate School for giving me the opportunity to study and work in such a fine program. Thanks to my fellow graduate students and colleagues, both past and present, for making the work environment pleasant and a home away from home. A special thanks to my parents for instilling in me the necessary values to succeed in life. And lastly, I thank my wife Rita for her support, love, and most of all, patience.

Chapter 1: Background and Introduction

L-Glutamate is widely accepted as the primary excitatory neurotransmitter in the mammalian central nervous system (CNS). It mediates both fast synaptic inter-neuronal communication and the more complex signal processing involved in learning, memory, and development (for review see Cotman et al., 1995). The ability of glutamate to participate in such a wide range of processes is a function of the excitatory amino acid (EAA) receptors that comprise the glutamatergic system. These receptors include subtypes that are coupled to ion channels (ionotropic) and second messenger systems (metabotropic). The ionotropic receptors were initially characterized and named according to the selective agonists N-methyl-D-aspartate (NMDA), α -amino-3-hydroxy-5-methyl-4-isoxazole propionate (AMPA), and kainate (KA). These classes include receptors which gate currents carried by Na^+ , K^+ , and Ca^{++} (for review see Monaghan and Cotman 1986). Metabotropic glutamate receptors are G-protein coupled to either cyclic adenosine monophosphate (cAMP) or to phosphoinositide (PI) second messenger systems. They were initially distinguished by the agonists 1-aminocyclo-pentane-*trans*-1,3-dicarboxylate (*trans*-ACPD) and L-2-amino-4-phosphonobutyrate (L-AP4), respectively (Conn and Pin, 1997). More recently, the employment of molecular techniques to clone these receptors,

and further pharmacological characterization has led to an even greater refinement in their sub-classification.

The inherent ability of glutamate to activate such a wide range of pharmacologically distinct receptors is dependent upon its acyclic structure. Free rotation is permitted about the $\alpha\beta$ and $\beta\gamma$ sp^3 bonds of glutamate, which allows it to assume stable low energy conformations in aqueous solution (Ham, 1974). This characteristic has been exploited in the design and discovery of conformationally constrained analogues of glutamate which selectively interact with these receptors and other components of the EAA system, such as the high-affinity sodium-dependent plasma membrane transporters (Chamberlin and Bridges, 1993; Chamberlin et al., 1998).

Following release from the presynaptic terminal, attenuation of the excitatory signal is accomplished by diffusion of glutamate from the synaptic cleft and its subsequent reuptake by high-affinity transporters located on neurons and surrounding glia. Analogous to the receptors, these transporters have been characterized according to differences in molecular structure and their relative affinities for selective substrates and inhibitors (Gegelashvili and Schousboe, 1997).

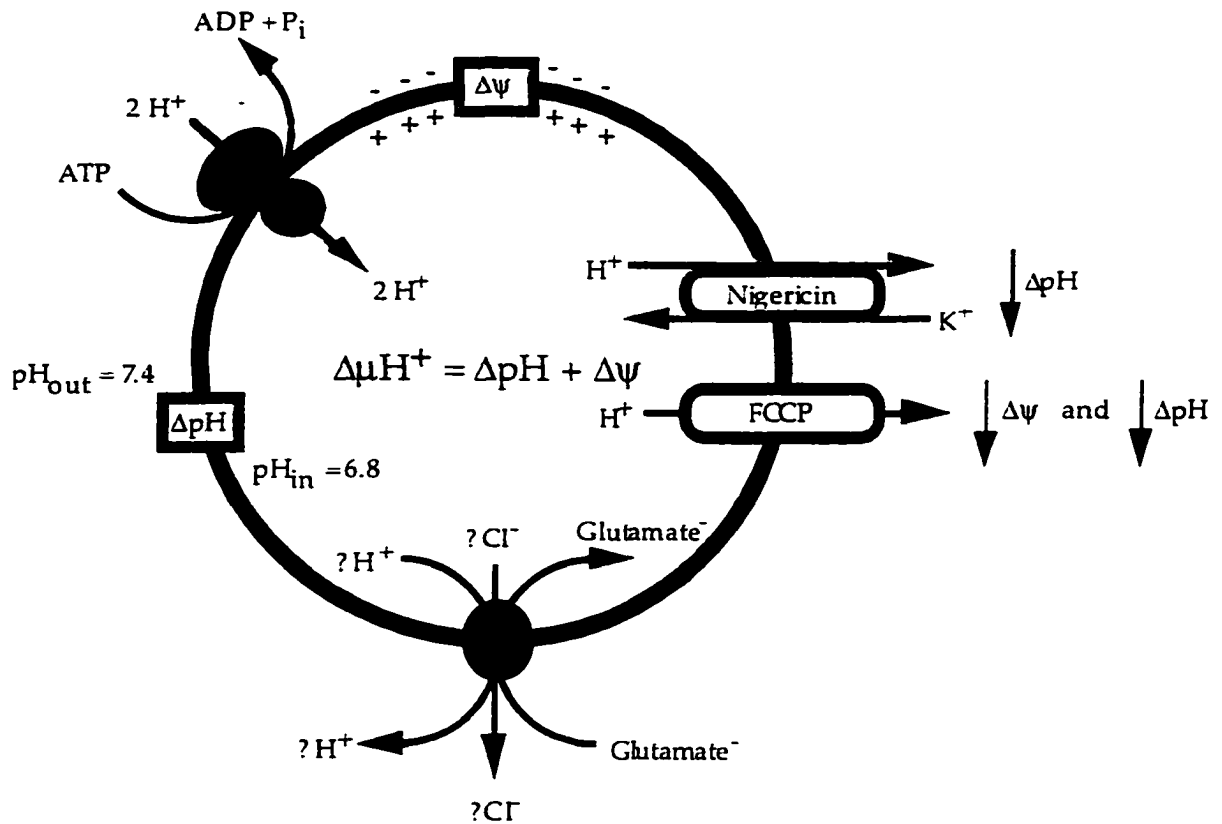
Although glutamate is today recognized as one of the most common CNS neurotransmitters, one criterion supporting this role remained elusive until the mid 1980's, namely its calcium-dependent release from synaptic vesicles. Before then, studies utilizing variable speed centrifugation and gel

filtration failed to show a substantial enrichment of glutamate and other amino acids in fractions of isolated synaptic vesicles (De Bellerocche and Bradford, 1973; De Bellerocche and Bradford, 1977). These findings contrasted with those of the biogenic amines (i.e., acetylcholine, norepinephrine, epinephrine, dopamine, and serotonin), which were found in high quantities using the same isolation techniques. Consequently, it was speculated that upon neuronal depolarization, glutamate may be released directly from the cytosol into the synapse, rather than from synaptic vesicles, as purported for other neurotransmitter systems (De Bellerocche and Bradford, 1977). This controversy was later resolved by two independent lines of investigation. First, it was demonstrated that glutamate released in a Ca^{++} -dependent manner originates from a non-cytosolic pool (Nicholls and Sihra, 1986). Second, it was shown that glutamate accumulation into synaptic vesicles is energy dependent (Naito and Ueda, 1983; Naito and Ueda, 1985; Maycox et al., 1988). Moreover, efflux of the vesicular contents will occur if the electrochemical gradient is not maintained, which would explain the earlier failure to isolate synaptic vesicles containing glutamate (Carlson and Ueda, 1990). In contrast, the stability of acetylcholine and catecholamines in synaptic vesicles in the absence of ATP is thought to be due to an intravesicular complexation (McMahon, 1991).

Within the last 15 years, the bioenergetics of vesicular glutamate uptake have been extensively characterized (see Ozkan and Ueda, 1998).

Transport into synaptic vesicles is driven by an electrochemical proton gradient ($\Delta\mu_{H^+}$) which includes contributions from both a membrane potential ($\Delta\Psi$) and a transmembrane pH gradient (ΔpH) (Figure 1.1). This electrochemical gradient is generated by a vacuolar-type Mg^{++} -dependent H^+ -ATPase which utilizes energy produced from the hydrolysis of cytosolic ATP to direct a flow of protons into the lumen of synaptic vesicles. The resulting charge differential (inside positive) leads to the formation of a $\Delta\Psi$ across the vesicular membrane. In the presence of permeant anions (e.g., Cl^-), $\Delta\Psi$ will diminish with the influx of negative ions and the net accumulation of HCl leading to an increase in ΔpH . Studies have shown that both $\Delta\Psi$ and ΔpH participate in vesicular glutamate uptake under physiological conditions, although their relative contributions to the uptake process remain to be clarified (Maycox et al., 1988; Tabb et al., 1992; Hartinger and Jahn, 1993). Therefore, compounds reducing either $\Delta\Psi$, ΔpH or both have been found to be effective non-competitive inhibitors of glutamate transport into synaptic vesicles. The effects of such compounds (e.g. nigericin and carbonyl cyanide *p*-trifluoromethoxyphenyl-hydrazine, (FCCP)) on the electrochemical proton gradient are also illustrated in Figure 1.1. Nigericin exchanges H^+ for K^+ ions across the vesicular membrane and, therefore, reduces ΔpH without affecting $\Delta\Psi$. FCCP reduces both ΔpH and $\Delta\Psi$ by equilibrating protons across the

Figure 1.1 Putative model of the bioenergetics of vesicular glutamate uptake (modified from Ozkan and Ueda, 1998).



vesicular membrane. In each case, micromolar concentrations of these compounds are able to effectively reduce the driving force for vesicular uptake and consequently attenuate glutamate accumulation (Tabb et al., 1992; Burger et al., 1989; Maycox et al., 1988; Naito and Ueda, 1985).

In addition to its contribution to the formation of ΔpH , Cl^- has been proposed to play a modulatory role in vesicular glutamate uptake by binding to a specific site on the transporter protein. It was reported that 4,4'-diisothiocyanatostilbene-2,2'-disulfonic acid (DIDS), a general anion channel blocker, could inhibit the Cl^- -dependent uptake and efflux of glutamate, and that this inhibition could be overcome with an excess amount of Cl^- , but not with another anion, such as glutamate (Hartinger and Jahn, 1993). This result could be explained by the presence of a Cl^- binding site on the intravesicular surface of the transporter, which may function to bind and exchange luminal Cl^- for cytosolic glutamate during uptake. Such a counter transport system may even be energetically favorable, acting to balance the negative charge gradient across the membrane. Unfortunately, a counter transport of Cl^- ions via the transporter itself or a separate chloride conducting site has not yet been directly demonstrated, owing in part to the high non-specific permeability of biological membranes to Cl^- .

Despite the finding that vesicular glutamate uptake is dependent upon $\Delta\mu\text{H}^+$, current evidence does not adequately explain how ΔpH and $\Delta\Psi$ regulate or drive this uptake process. In regard to data indicating that H^+

efflux is coupled to glutamate uptake, it has been suggested that a 1:1 counter exchange of these molecules is energetically feasible (Shioi and Ueda, 1990). Additionally, it is quite plausible that the intravesicular acidification resulting from H^+ and Cl^- accumulation, might significantly change the conformation of the transport protein due to protonation/deprotonation of ionizable amino acid residues (Tabb et al., 1992). While the ΔpH component of $\Delta \mu H^+$ at physiological Cl^- concentrations (4 mM) is relatively small ($\Delta pH = 0.6$), such a change in intravesicular pH could have substantial effects on the conformation and activity of the transporter.

Following the demonstration of energy-dependent glutamate uptake by synaptic vesicles, numerous studies were aimed at delineating the pharmacology and kinetic properties of this transport system. As a result, key differences were identified that differentiated the vesicular and cellular glutamate transporters. First, vesicular transport is driven by an electrochemical proton gradient, stimulated by physiologically relevant concentrations of Cl^- , and is Na^+ -independent. In contrast, cellular transport predominantly responds to Na^+ and K^+ gradients ($Na^+_o > Na^+_i$; $K^+_o < K^+_i$). Secondly, affinity for the endogenous substrate L-glutamate dramatically differs between the two systems. Thus, K_m values for vesicular uptake are in the 1-3 mM range (Naito and Ueda, 1985), whereas the K_m values for the high-affinity cellular uptake system vary from 5-50 μM (Bridges et al., 1994; Garlin et al., 1995). This difference in affinity may reflect the relative concentrations

of glutamate inside and outside of the cell and the fact that a high-affinity uptake system may not be required by synaptic vesicles because cytosolic glutamate levels are in the millimolar range (Maycox et al., 1990). Finally, the specificities of the two transport systems are also distinct, as a number of well known substrates and inhibitors of cellular transporters exhibit little or no activity in the vesicular system (e.g. D-, L-cysteic acid, D,L-threo- β -hydroxyaspartic acid, L-*trans*-2,4-PDC, etc.; Table 6.1).

Presently, pharmacological characterization of the vesicular glutamate pharmacophore is still in its infancy. Initial studies included compounds previously reported to interact with other components of the EAA system, thereby addressing their potential cross-reactivities with vesicular uptake. In general, these studies met with marginal success, although a few potentially interesting compounds were indentified. For example, kynurenic acid, a non-selective inhibitor of EAA ionotropic receptors, and *trans*-ACPD, a metabotropic receptor agonist, were both reported to competitively inhibit vesicular glutamate uptake with K_i values less than that of glutamate itself (Fyske et al., 1992; Winter and Ueda, 1993). Even more potent inhibitors were discovered when several high molecular weight organic dyes, originally shown to antagonize EAA receptor binding (i.e. trypan blue, Evans Blue, and Chicago Sky Blue), were tested as transport inhibitors (Roseth et al., 1995; Roseth et al., 1998). These compounds inhibit vesicular glutamate uptake at nanomolar concentrations. Very recently, the inhibitory activity was also

characterized for an endogenous substance, termed inhibitory protein factor (IPF), which is derived from the cytoskeletal protein fodrin (Ozkan et al., 1997). At nanomolar concentrations, IPF inhibits both glutamate and GABA uptake by synaptic vesicles and is proposed to play an *in vivo* modulatory role in vesicular transport.

Although the number of identified inhibitors is increasing, little is known concerning their molecular interactions with the transporter site or, how they mimic the substrate binding conformation of L-glutamate. The work introduced in this study begins to address these questions. Two distinct series of compounds are presented which competitively inhibit vesicular glutamate uptake. One is based upon a quinoline core framework, and the other a naphthalene ring system. Detailed kinetic analyses and molecular modeling studies were utilized to rationalize the inhibitory activities of these compounds at the vesicular site. Moreover, further insight into the mechanism of vesicular glutamate transport is made and a method for the rapid differentiation of substrates from non-substrates is presented.

Chapter 2: Methods and Materials

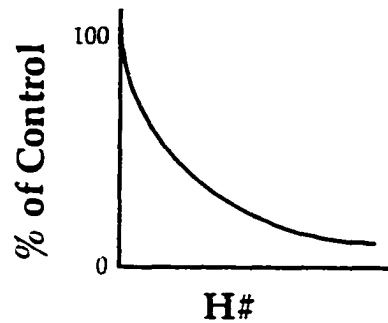
Isolation of synaptic vesicles

Synaptic vesicles were isolated from the forebrains of male Sprague-Dawley rats (200-300 g) essentially as described by Kish et al., (1989). Briefly, rats were rapidly decapitated and their cerebrums were removed and minced with scissors in an ice-cold solution consisting of 0.32 M sucrose, 1.0 mM sodium bicarbonate, 1.0 mM magnesium acetate, and 0.5 mM calcium acetate (pH 7.2). The finely minced cerebrums were homogenized (motorized Potter-Elvehjem, Teflon/glass (Wheaton)) and centrifuged (12,000 *g*_{max}, 15 min, Sorval SS-34 rotor), after which the resulting pellet was resuspended in a 6.0 mM Tris-maleate buffer (pH 8.1). Following a 45 min incubation at 4⁰C, the suspension was centrifuged (43,000 *g*_{max}, 15 min, Sorval SS-34 rotor). The collected supernatant was re-centrifuged (222,000 *g*_{max}, 55 min, Beckman Ti 60 rotor) and the resulting pellet resuspended by homogenization in 0.32 M sucrose, 1.0 mM sodium bicarbonate, and 1.0 mM dithiothreitol (pH 7.2). Synaptic vesicles prepared in this manner and stored at -80 ⁰C exhibited similar levels of glutamate uptake activity for at least 2 weeks.

Assay and kinetic analyses of vesicular glutamate transport:

The uptake of glutamate into synaptic vesicles was quantified using a modification of the procedure described by Kish et al., (1989). Synaptic vesicles were resuspended by vortexing in a buffer containing 5.0 mM MgCl₂, 375 mM sucrose, and 5.0 mM N-[2-hydroxyethyl]piperazine-N'-[2-ethanesulfonic acid] (HEPES) (pH 7.4) and maintained at 4⁰C. Vesicles (80 μL, 100-150 μg protein) were preincubated for 5 min at 30⁰C. Uptake was initiated by the addition of a concentrated stock solution (20 μL, 30⁰C) that yielded a final assay mixture of (0.25 - 8.0 mM L-[3,4-³H]-glutamate, 2.0 mM ATP, 4.0 mM MgCl₂, 4.0 mM KCl, 300 mM sucrose, and 5.0 mM HEPES (pH 7.4). Where indicated, inhibitors were added to the assays in combination with ³H-L-glutamate. Following a 1.5 min incubation, uptake was terminated by the addition of 3.0 mL of ice cold 150 mM KCl followed immediately by rapid vacuum filtration (<10 psi) through Millipore HAWP filters (25 mm, 0.45 μm). Assay tubes and filters were sequentially rinsed twice more with 3.0 mL of ice cold 150 mM KCl. The filters were transferred to 5.0 mL glass scintillation vials and 3.5 mL Liquiscint scintillation fluid (National Diagnostics) was added to each. Radioactivity retained on filters was quantified by liquid scintillation counting (LSC, Beckman LS 6500). In the instance of certain dye containing assays, colorimetric quenching artificially

decreased the amount of measured radioactivity. For these samples, corrections were made to account for this reduction, utilizing a one-phase exponential decay equation to describe the relationship between the degree of quenching (H#) and the reduction in measurable radioactivity (% of Control) (refer to following illustration).



Nonspecific uptake, binding, or leakage was corrected for by subtracting $^3\text{H-L}$ -glutamate accumulated in the absence of ATP. Typically, the non-ATP-dependent component was less than 20% of the ATP-dependent value. Initial experiments established that under the assay conditions employed, glutamate uptake into the synaptic vesicles was linear with respect to both time and protein content (data not shown). Lineweaver-Burk plots and associated kinetic parameters were estimated by computer analysis (K•CAT kinetic program, BioMetallics Inc.) with weighting based on constant relative error. The resulting K_i values were estimated on the basis of a replot of $K_{m, app}$ values. Sigmoidal dose-response curves and IC_{50} values were determined from non-linear regression analyses of a one-site competition model (PRISM program, GraphPad Software, Inc.). Reported K_i values were estimated from

IC_{50} values according to the Cheng-Prusoff relationship (Cheng and Prusoff, 1973) for competitive inhibitors (refer to the following equation).

$$K_i = \frac{IC_{50}}{1 + \frac{[\text{substrate}]}{K_m}}$$

Protein concentrations were determined by the Pierce BCA assay (bicinchoninic acid; Smith et al., 1985).

Vesicular ATP-dependence of $^3\text{H-L-glutamate}$ uptake and retention

In one series of experiments transport assays were modified to specifically examine the dependence of $^3\text{H-L-glutamate}$ uptake on ATP. In these studies, ATP concentrations were varied from 2-6 mM, and the vesicle content of the assay was increased 4-5 fold. Instead of terminating an individual assay for each time point, aliquots (25 μL) were removed at the indicated times from a common incubation and terminated by diluting in 3 mL of ice cold 150 mM KCl, immediately followed by vacuum filtration and rinsing (2 x 3 mL). Radioactivity retained on filters was quantified as previously described.

Efflux of glutamate from synaptic vesicles

Synaptic vesicles were first incubated with ^3H -L-glutamate under the same conditions used to quantify uptake. Following a 5 min incubation, vesicles (100 μL) were diluted 20-fold into incubation buffer devoid of ATP, but containing unlabeled L-glutamate and/or an inhibitor at the indicated concentrations. These assays were then allowed to incubate at 30°C for the indicated times and efflux was terminated by the addition of ice cold 150 mM KCl (3 mL), immediately followed by vacuum filtration and rinsing (2×3 mL) as described earlier. Radioactivity retained on filters was quantified by LSC.

Synaptic plasma membrane preparation and receptor binding assay

Synaptic plasma membranes (SPMs) were prepared from male Sprague-Dawley rat forebrains by differential centrifugation and assayed for radioligand binding as described by Bridges et al., (1989). Binding assays were carried out using optimally selective conditions of time, temperature, and buffer for each of the three glutamate ionotropic receptor classes. To quantify N-methyl-D-aspartate (NMDA) receptor binding, SPMs were incubated with L-[3,4- ^3H]-glutamate (10 nM, 41 Ci/mmol) in 50 mM Tris-acetate, pH 7.2, at 4°C for 10 min (Monaghan and Cotman, 1986). Kainate (KA) receptor binding was

quantified by incubating SPMs with $^3\text{H-KA}$ (10 nM, 58 Ci/mmol) in 50 mM Tris-citrate buffer, pH 7.0, at 4°C for 30 min (Simon et al., 1976; London and Coyle, 1979), AMPA receptor binding was measured with $^3\text{H-AMPA}$ (10 nM, 27.6 Ci/mmol) in 50 mM Tris-acetate buffer, pH 7.2, containing 100 mM KSCN for 30 min at 4°C (Honore et al., 1982). Nonspecific binding was determined in each of the assays by the inclusion of 200 μM NMDA, 100 μM KA, or 100 μM quisqualate respectively. Values represent specific binding and are reported as the percentage of control binding (mean \pm SEM; n = number of triplicates).

Synaptosome preparation and Na^+ -dependent D-aspartate transport

Rat forebrain synaptosomes were prepared from male Sprague-Dawley rats using a discontinuous Ficoll gradient essentially as described by Booth and Clark (1978). The synaptosomal pellet was suspended in assay buffer at a final concentration of about 0.2 mg protein/mL. Uptake of $^3\text{H-D-aspartate}$ (5 μM) was measured in assay buffer containing 128 mM NaCl, 10 mM glucose, 5 mM KCl, 1.5 mM NaH_2PO_4 , 1 mM MgSO_4 , 1 mM CaCl_2 , and 10 mM Tris (pH 7.4) (Kuhar and Zarbin, 1978). Following a 5 min preincubation at 25°C ,

uptake was initiated by the simultaneous addition of ^3H -D-aspartate and inhibitors. Uptake was allowed to proceed for 2 min after which the reaction was quenched with 6 mL of ice cold buffer and rapidly filtered onto Whatman GF/F glass fiber filters. Following a rinse with ice cold buffer, the retained radioactivity was quantified by LSC. All values were corrected for background by subtracting ^3H -D-aspartate accumulated at 4°C . Previous experiments have demonstrated that uptake under these conditions is linear with respect to both protein content and time.

Materials

L-Glutamic acid, kynurenic acid, 7-chloro-kynurenic acid, picolinic acid, 4-hydroxy-pyridine, quinaldic acid, xanthurenic acid, Evans Blue, and carbonyl cyanide p-trifluoromethoxyphenylhydrazone (FCCP) were purchased from Sigma (St. Louis, MO.). Pyridine, 3-hydroxy-picolinic acid, quinaldic acid, quinoline, 4-hydroxy-quinoline, 2-pyrazine carboxylic acid, Chicago Sky Blue, 4-amino-5-hydroxy-1-naphthalene sulfonic acid, Congo Red, 4-amino-1-naphthalene sulfonic acid, 1-naphthol-3,6-disulfonic acid, Naphthol Blue Black, Nitro Red, and 4-amino-5-hydroxy-2,7-naphthalene disulfonic acid were purchased from Aldrich (Milwaukee, WI). Chicago acid, Gallion, Azophloxine, and Chromotrope 2R were purchased from TCI America

(Portland, OR). 4-Hydroxy-picolinic acid was synthesized as previously described by Clark-Lewis and Mortimer (1961). L-[3,4-³H]-Glutamic acid, [vinylidine-³H]-kainic acid, D,L- α -[5-methyl-³H]-AMPA, and D-[2,3-³H]-aspartic acid were obtained from Dupont NEN (Boston, MA). All other reagents were obtained from Sigma.

Chapter 3: Vesicular pharmacology of quinoline and pyridine based inhibitors

Introduction

While large numbers of excitatory amino acid (EAA) analogues have been tested as potential blockers of vesicular glutamate uptake, only a few potent competitive inhibitors have been identified; e.g., *trans*-1-aminocyclopentane-1,3-dicarboxylic acid (*trans*-ACPD) (Winter and Ueda, 1993), bromocriptine (Carlson et al., 1989), certain naphthalene disulfonic acids (Roseth et al., 1995), and kynurenate (Fyske et al., 1992). This last compound is of particular interest because it is not only present in the CNS (for review see Stone, 1993) but also because it exhibits activity at EAA ionotropic receptors. Specifically, kynurenate acts as a competitive inhibitor at the glutamate sites on the NMDA, KA and AMPA receptors (Ganong et al., 1983), and at the glycine site on the NMDA receptor (Kessler et al., 1989; Watson et al., 1988).

The work presented in this chapter details an analysis of the structure-activity relationships and kinetic properties of a panel of kynurenate analogues as inhibitors of the vesicular glutamate transporter. Further, two closely related derivatives of kynurenate, 7-chloro-kynurenate and

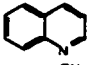

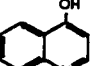

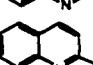

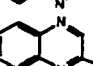
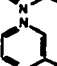
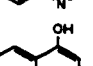
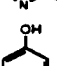
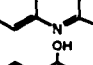
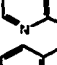
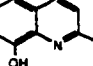
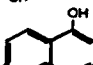
xanthurenate, are identified that are markedly more potent as uptake inhibitors than the parent compound. Parallel studies assessed the activity of these inhibitors at the sodium-dependent synaptosomal transporter and at the EAA ionotropic receptors. Computer-based molecular modeling was used to analyze the structure-activity data in an attempt to explain the inhibitory activities of these compounds and identify the active conformations of glutamate that bind to the vesicular transporter. The findings will help to further define the pharmacological specificity of the glutamate binding site on the vesicular uptake system and identify novel pharmacological probes with which to investigate its function.

Results

Pharmacology of the vesicular glutamate transporter

A series of quinoline and pyridine analogues of kynurenate were tested for their ability to inhibit the uptake of ^3H -L-glutamate into synaptic vesicles prepared from rat forebrain (Table 3.1). Consistent with previous studies (Fyske et al., 1992), kynurenate markedly reduced the uptake of ^3H -L-glutamate (0.25 mM) to 11% of control values (1532 ± 111 pmol/min/mg protein) when included in the assay at 5.0 mM. Analogues of kynurenate

Table 3.1 Inhibitory activities of kynurenate analogues on the vesicular uptake of L-glutamate

Compound	Structure	Vesicular Uptake of ³ H-L-Glutamate (% of Control)	Compound	Structure	Vesicular Uptake of ³ H-L-Glutamate (% of Control)
<i>Quinoline and Quinoxaline Analogues</i>			<i>Pyridine and Pyrazine Analogues</i>		
Quinoline		56 ± 4 (5)	Pyridine		91 ± 2 (3)
4-OH-Quinoline		61 ± 2 (4)	4-OH-Pyridine		98 ± 9 (3)
Quinaldate		34 ± 3 (5)	Picolinate		86 ± 3 (5)
2-Quinoxaline carboxylate		14 ± 1 (3)	2-Pyrazine carboxylate		90 ± 3 (3)
Kynurenate		11 ± 1 (15)	4-OH-Picolinate		79 ± 8 (3)
Xanthurenate		4 ± 1 (12)	3-OH-Picolinate		27 ± 3 (6)
7-Cl-Kynurenate		2 ± 1 (6)			
4-Methoxy-2-quinoline carboxylate		25 ± 1 (4)			

The vesicular uptake of ³H-L-glutamate (0.25 mM) was performed as described in Chapter 2. Kynurenic acid analogues were present in the incubation medium at a final concentration of 5mM. Results are reported as a percentage of control uptake ± SEM with n number of experiments in parentheses. The control value for glutamate uptake was 1532 ± 111 pmol/min/mg protein (n = 49).

were selected in an effort to examine the contribution of the carboxylate and the hydroxy moieties to the process of substrate binding. Thus, 4-hydroxyquinoline, which lacks the 2-carboxylate group of kynurenate, and quinaldate, in which the 4-OH moiety is absent, proved to be less effective than kynurenate, reducing uptake to approximately 60% and 30% of control, respectively. Interestingly, when both functional groups were absent, as in quinoline, some inhibitory activity was retained. Replacing the 4-OH moiety with a methoxy group (4-methoxy-2-quinoline carboxylate) or embedding a N atom at the 4-position of the hetero-ring (2-quinoxaline carboxylate) resulted in inhibitory activities that were more comparable to that of kynurenate. Marked increases in inhibitory activity were observed in those analogues in which electron donating groups (*e.g.*, OH, Cl) were added to the aryl ring of kynurenate. Thus, both xanthurenate and 7-Cl-kynurenate almost completely abolished the uptake of ^3H -L-glutamate (0.25 mM) into the synaptic vesicles when included in the assays at 5.0 mM.

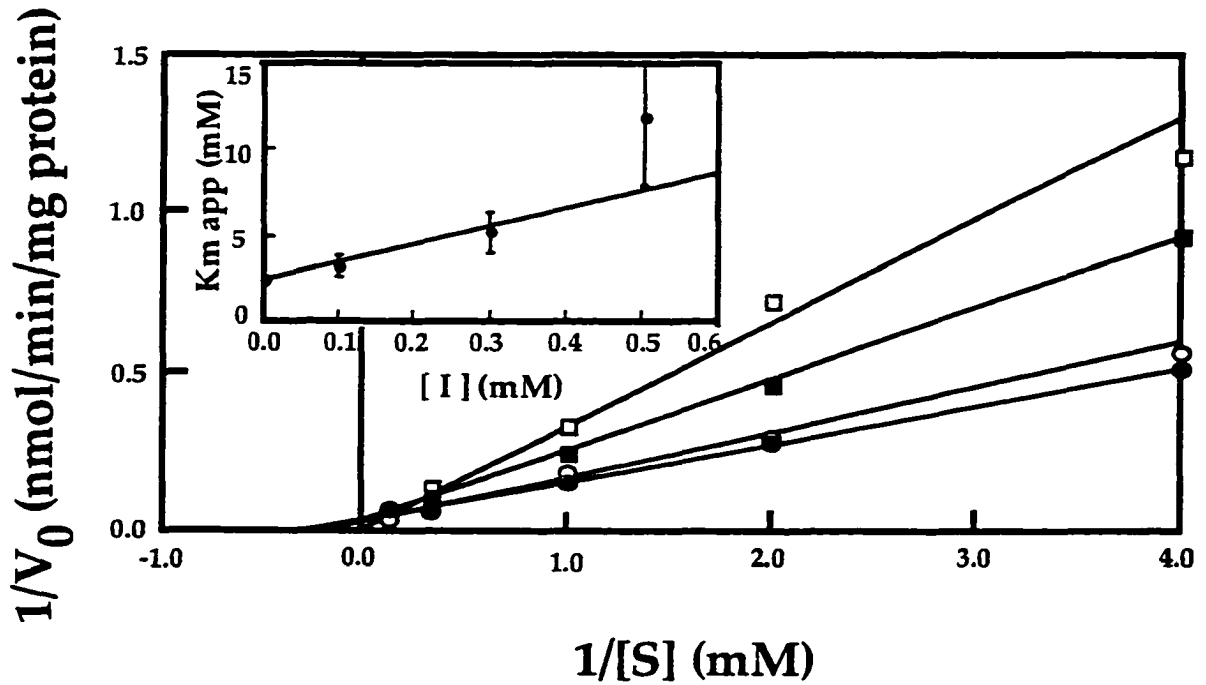
In contrast to the activities of the quinoline and quinoxaline derivatives, the mono-heterocyclic analogues exhibited little or no inhibitory activity. Included among these compounds was 4-OH picolinate, which is structurally identical to the hetero-aryl ring of kynurenate. The exception to this pattern was 3-OH picolinate (5.0 mM), which reduced the uptake of ^3H -L-glutamate (0.25 mM) into the synaptic vesicles to 27% of control.

More detailed kinetic studies were carried out on those analogues identified in Table 3.1 as potent inhibitors of vesicular uptake. A representative Lineweaver-Burk plot for the inhibition of vesicular glutamate transport by xanthurenate is illustrated in Figure 3.1. The K_m and V_{max} values for the transport of L-glutamate were found to be 2.77 ± 0.15 mM and 24.86 ± 2.06 nmol/min/mg protein (n=26), respectively. The patterns of inhibition observed with xanthurenate, as well as with the other compounds analyzed, were all consistent with actions of competitive inhibitors. Values for K_i were determined on the basis of a replot of $K_{m,app}$ values (inset Figure 3.1; Table 3.2) which, in the instance of xanthurenate, was found to be 0.19 ± 0.04 mM (n=6). When L-glutamate was tested in this manner the K_i value obtained (1.63 ± 0.21 mM) was similar to its observed K_m . Consistent with the initial assays of inhibitory activity, xanthurenate and 7-Cl-kynurenate proved to be the most potent inhibitors, exhibiting K_i values markedly less than the endogenous substrate L-glutamate (Table 3.2).

Pharmacological specificity of kynurenate analogs

Those compounds identified as potent inhibitors of vesicular glutamate uptake were also evaluated for their ability to block: *i*) the transport of ^3H -D-aspartate into rat forebrain synaptosomes and *ii*) the binding of

Figure 3.1 Demonstration of the competitive inhibition by xanthurenate on ^3H -L-glutamate uptake into synaptic vesicles.



Representative Lineweaver-Burk plot of a single experiment demonstrating competitive inhibition by xanthurenate (0.1, 0.3, 0.5 mM) on the uptake of ^3H -L-glutamate (0.25 - 8.0 mM) into rat brain synaptic vesicles. The above plots yielded a control $V_{max} = 20.99 \pm 1.33$ nmol/min/mg protein and $K_m = 2.46 \pm 0.23$ mM. Inset shows a replot of K_m apparent *versus* xanthurenate concentration producing a $K_i = 0.24 \pm 0.06$ mM.

Table 3.2. Kinetic analyses of kynurenic acid analogues as competitive inhibitors of $^3\text{H-L-glutamate}$ uptake into synaptic vesicles.

Compound	$K_i \pm \text{SEM}$
L-Glutamate	1.63 mM \pm 0.21 (5)
3-OH-Picolinate	1.58 mM \pm 0.21 (3)
Kynurenate	1.28 mM \pm 0.19 (4)
2-Quinoxaline carboxylate	0.70 mM \pm 0.07 (3)
7-Cl-Kynurenate	0.59 mM \pm 0.14 (5)
Xanthurenate	0.19 mM \pm 0.04 (6)

Vesicular glutamate uptake was determined essentially as described in Chapter 2 with the exception that $^3\text{H-L-glutamate}$ concentrations were varied from 0.25 - 8.0 mM in the presence of three different concentrations of inhibitor. K_i values were estimated on the basis of a replot of $K_{m, app}$ values and are reported as mean $K_i \pm \text{SEM}$, with n number of experiments in parentheses.

radioligands to the EAA ionotropic receptors on rat forebrain synaptic plasma membranes (SPMs). When included in the synaptosomal transport assays at 250 μM , the kynurenate derivatives failed to attenuate the uptake of ^3H -D-aspartate (5 μM) (Table 3.3). In contrast, both L-glutamate and L-aspartate produced an almost complete inhibition. Consistent with distinct specificities, D-aspartate did not inhibit the uptake of ^3H -L-glutamate into the synaptic vesicles (data not shown). While synaptosomes have historically been considered to represent presynaptic transport, recent pharmacological data (e.g., sensitivity to dihydrokainate) suggest that uptake in this preparation may include a significant contribution from glial systems (Arriza et al., 1994). Thus, while the kynurenate analogues exhibited no inhibitory activity, further resolution of neuronal *vs* glial activity requires additional studies.

The analogues were then assessed for their ability to block the binding of ^3H -L-glutamate (10 nM), ^3H -kainate (10 nM), and ^3H -AMPA (10 nM) to NMDA, KA and AMPA receptors, respectively. The results of these binding studies are summarized in Table 3.4 as percent of control: 0.19 ± 0.02 pmol/mg protein for ^3H -L-glutamate, 0.27 ± 0.04 pmol/mg protein for ^3H -kainate, and 0.13 ± 0.01 pmol/mg protein for ^3H -AMPA. As expected, kynurenate (100 μM) and 7-Cl-kynurenate (100 μM) inhibited the binding of all three radioligands. In contrast, xanthurenate, which proved to be the most potent vesicular

Table 3.3 Activity of kynurenate analogs in inhibiting the uptake of $^3\text{H-D-}$ aspartate into synaptosomes isolated from rat forebrain.

Compound	Concentration (μM)	Inhibition of Synaptosomal $^3\text{H-D-Aspartate}$ Uptake (% of Control)
L-Glutamate	250	0
L-Aspartate	250	2 ± 2 (5)
Kynurenate	250	103 ± 3 (5)
7-Chloro-kynurenate	250	100 ± 6 (5)
Xanthurenate	250	102 ± 2 (5)
3-Hydroxy-picolinate	250	104 ± 2 (5)
4-Hydroxy-picolinate	250	96 ± 3 (3)
2-Quinoxaline carboxylate	250	104 ± 2 (5)
Quinaldate	250	101 ± 1 (5)

The abilities of the compounds listed above to block the uptake of $^3\text{H-D-}$ aspartate ($5 \mu\text{M}$) into rat forebrain synaptosomes was determined as described in Chapter 2. Results are reported as the mean \pm SEM of the percentage of control uptake (2.86 ± 0.28 nmol/min/mg protein) with n number of experiments in parentheses.

Table 3.4 Pharmacological specificity of kynurenic acid analogues as inhibitors of EAA ionotropic receptor binding.

Compound	³ H-L-GLU binding to NMDA receptors (% of Control)	³ H-AMPA binding to AMPA receptors (% of Control)	³ H-KA binding to KA receptors (% of Control)
Kynurenate	41 ± 2 (4)	58 ± 7 (4)	72 ± 6 (3)
7-Chloro-kynurenate	39 ± 2 (4)	33 ± 7 (4)	62 ± 3 (3)
Xanthurenate	78 ± 3 (4)	84 ± 10 (4)	91 ± 10 (3)

EAA ionotropic receptor binding was selectively assayed as described in Chapter 2. Kynurenate analogues were included in the assay at a concentration of 100 µM. All values represent specific binding and are reported as the means of the percentage of control binding ± SEM (see text), with *n* number of experiments in parentheses.

transport blocker, produced much less inhibition of ^3H -L-glutamate (22%) and ^3H -AMPA (16%) binding and exhibited little or no effect on ^3H -KA binding.

Discussion

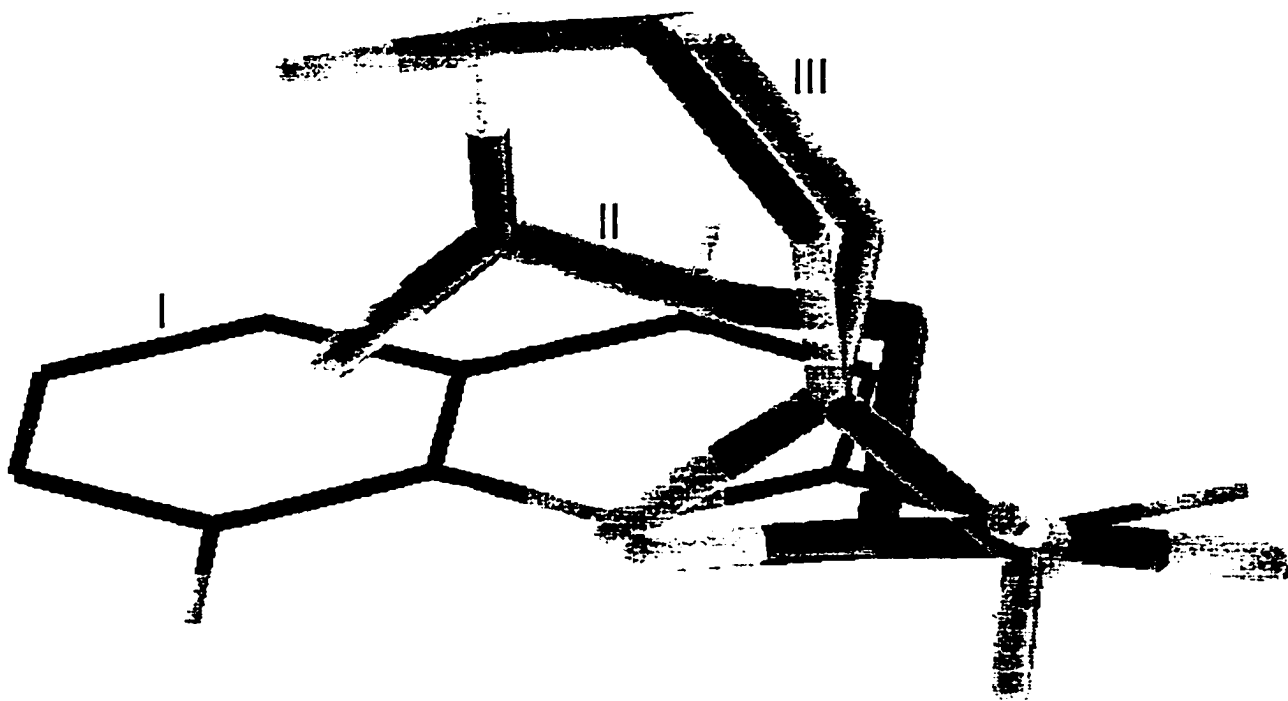
The identification of kynurenate as an inhibitor of glutamate uptake into synaptic vesicles prompted our investigation into the structure-function relationships governing this activity (Fyske et al., 1992). The demonstration that several of the substituted quinolines are competitive inhibitors and exhibit K_i values lower than L-glutamate itself is consistent with their binding to the substrate site on the transporter and raises intriguing questions as to the chemical/conformational basis of their ability to mimic the binding of glutamate to the transport protein. While a few compounds have been identified as more potent inhibitors (e.g., naphthalene-disulfonic acid dyes, Roseth et al., 1995), the greater structural similarities with L-glutamate (e.g., possession of an α -nitrogen and α -carboxylate) allows for a more direct analysis of glutamate binding. In the instance of the kynurenate derivatives, direct comparison of the molecules would suggest that the ring nitrogen and 2-carboxylate of kynurenate most likely correspond to the α -amino and α -carboxylate moieties of glutamate, respectively. The identification of the

analogous distal carboxylate mimic is however, less straight forward. Although the positioning of the 4-OH group of kynurenate places it at an appropriately relevant distance from the proximal carboxylate, its pKa of 10.5 indicates that there is little chance that it will be ionized at physiological pH (Robinson et al., 1985). Rather than a specific functional group mimicking the presence of this second acidic group, we hypothesize that the electron density associated with the conjugated aryl ring may be sufficient to mimic the negative charge of the distal carboxylate. This process would be analogous to the well known ability of aryl rings to electrostatically interact with positively charged functional groups of proteins (e.g., arginine and lysine). Such a relationship is supported by both the inhibitory potency of quinaldate and 2-quinoxaline carboxylate, which lack the hydroxyl moiety, and the lack of activity of the substituted monocyclic pyridine analogues, particularly 4-OH picolinate. Further evidence that the second ring system may provide a requisite negative character rests with the two quinoline analogues that proved to be more potent than kynurenate, xanthurenate and 7-Cl-kynurenate. In both cases, the substituents present on the aryl rings of these analogues (OH and Cl, respectively) are considered electron donating and would increase the electron density of the ring. If properly oriented, this increase in electron density may more closely approximate the negative charge of the distal carboxylate and explain the greater effectiveness of xanthurenate and 7-Cl-kynurenate as inhibitors.

To explore this possibility in more detail, we carried out a series of computer-based molecular modeling studies (SYBYL modeling program; TRIPOS Inc.; St. Louis, MO) with L-glutamate, xanthurenate and (1R,3S)-ACPD (previously identified as an inhibitor; Winter and Ueda, 1993). The strategy employed was to first identify minimized conformations of the individual molecules and then compare the spatial positioning of their functional groups (i.e., α -amino, α -carboxyl, and distal carboxyl groups) in a three point best fit analysis to identify conformers exhibiting the greatest degree of overlap (Chamberlin et al., 1998). In the instance of L-glutamate, the resulting minimized structures are similar to nine stable solution conformers previously identified in NMR analyses (Ham, 1974; Chamberlin and Bridges, 1993). The modeling process was also simplified by the fact that xanthurenate, as well as the other quinoline derivatives, are conformationally locked planar molecules. Since xanthurenate does not possess a distal acidic group, the regions of maximum electron density above and below the aryl ring were designated as the distal carboxylate mimics. Thus, the modeling was performed by fitting the charged groups of minimized L-glutamate conformers (i.e., the nitrogen, α -carboxylate carbon, and distal carboxylate) with the proposed functional moieties of xanthurenate (the nitrogen, 2-carboxylate carbon, and aromatic ring electron density).

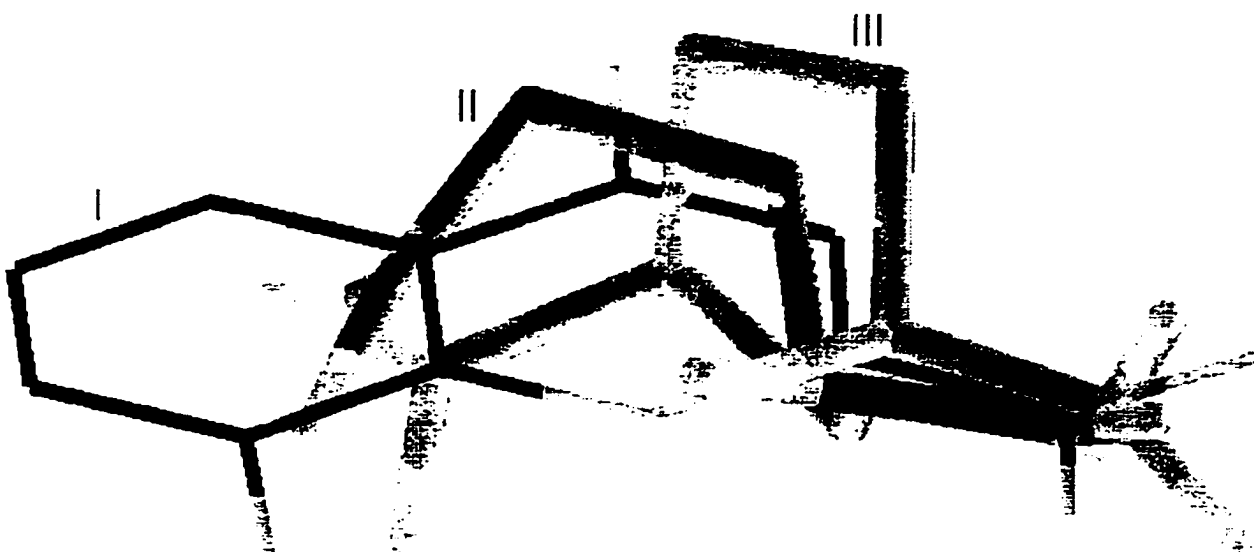
The resulting comparisons of L-glutamate and xanthurenate (Figure 3.2 and 3.3) yielded two conformations of L-glutamate with a relatively high

Figure 3.2 Depiction of the overlap of the distal carboxylates of L-glutamate and (1R,3S)-ACPD with the electron density above the carbocyclic ring of xanthurenate.



Computer-based overlays of minimized conformations of xanthurenate (I), L-glutamate (II), and (1R, 3S)-ACPD (III) were performed as described in text. The molecules are aligned to achieve maximum overlap of the alpha-nitrogens, alpha-carbons, and electron densities of the aromatic ring and distal carboxylates. In this rendition, the overlap of the distal carboxylates and carbocyclic ring electron density is shown occurring above the aromatic ring.

Figure 3.3 Depiction of the overlap of the distal carboxylates of L-glutamate and (1R,3S)-ACPD with the electron density below the carbocyclic ring of xanthurenate.



Computer-based overlays of minimized conformations of xanthurenate (I), L-glutamate (II), and (1R, 3S)-ACPD (III) were performed as described in text. The molecules are aligned to achieve maximum overlap of the alpha-nitrogens, alpha-carbons, and electron densities of the aromatic ring and distal carboxylates. In this rendition, the overlap of the distal carboxylates and carbocyclic ring electron density is shown occurring below the aromatic ring.

degree of overlap: one positioning the distal carboxylate above the aromatic ring (Figure 3.2; RMS deviation of 0.278 Å) and one locating the distal carboxylate below the aromatic ring (Figure 3.3; RMS deviation of 0.692 Å). Of the two glutamate conformations, the one pictured in Figure 3.2 also exhibits a greater overlap with xanthurenate in regard to the positioning of its carbon backbone, particularly the α , β and γ carbon atoms. Analogous comparisons with (1R,3S)-ACPD identified a single minimized “cupped” conformer that could be positioned with the distal carboxylate either above (Figure 3.2) or below (Figure 3.3) the aryl ring of xanthurenate: (RMS of 0.583 Å and 0.705 Å) in Figure 3.2 and 3.3, respectively). Interestingly, this “cupped” conformation of (1R,3S)-ACPD was also proposed as the active conformer in earlier modeling studies of metabotropic receptor binding (Chamberlin and Bridges, 1993). Even though the two proteins exhibit distinct pharmacologies, it is entirely possible that ACPD or other ligands bind to these two proteins in similar conformations. If this is the case, it would suggest that other factors (e.g., steric tolerance, hydrophilicity or hydrophobicity of the surrounding protein amino acids, or hydrogen-bonding capacity of the binding pocket) contribute to the respective specificities of the binding sites.

Beyond their value in modeling the binding site of the vesicular glutamate transporter, this library of quinoline- and pyridine-based inhibitors is of interest because it includes kynurenate and xanthurenate, two kynurenine metabolites endogenous to the mammalian CNS. The presence

of these compounds in the brain raises obvious questions as to whether or not they may influence the function of the vesicular uptake system *in vivo*. This issue is similar in many ways to the lengthy discussions that have also revolved around the potential inhibitory action of kynurenate at the EAA ionotropic receptors (Stone, 1993). In the instance of the vesicular glutamate transporter, however, the action of these metabolites would be dependent upon their accumulation in neurons, rather than the extracellular location required to interact with EAA receptors. Although our data indicate that the kynurenate derivatives do not inhibit the sodium-dependent synaptosomal glutamate transporter, it is unclear as to the relative contributions of neuronal or glial membranes to this process. Further, a lack of activity at these cellular transporters does not preclude the possibility that the compounds may be substrates of other uptake systems. Interestingly, it has also been suggested that the majority of kynurenate in the CNS is of glial origin (Wu et al., 1992). While the potential *in vivo* actions of kynurenate and xanthurenate within the EAA system remain to be resolved, these new inhibitors provide a valuable molecular framework for delineating the pharmacophore of the vesicular glutamate transporter and the design of more potent and selective uptake blockers.

Chapter 4: Inhibition of vesicular glutamate uptake by naphthalene sulfonic acid dyes

Introduction

In a previous study, two naphthylamine-based disulfonic acid dyes, Evans Blue and Chicago Sky Blue, were reported to competitively block the uptake of ^3H -L-glutamate into rat brain synaptic vesicles, with K_i values of 40 and 190 nM respectively (Fyske et al., 1992). As these dyes are apparently greater than 1000-fold more potent as inhibitors than the kynurenic acid analogues characterized in Chapter 3, it was decided to examine the inhibitory activities of these and similar compounds within this class in greater detail. A cursory examination reveals certain structural similarities between naphthylamine sulfonic acid dyes and kynurenic acid analogues. Most notably, both series of compounds incorporate a bicyclic 6-membered conjugated ring system as their core framework. Due to the rigidity of the adjoined aromatic rings, both frameworks are conformationally planar, which causes the functional group substitutions to be held in specific spatial orientations. In addition, each class of compounds includes substitutions (e.g. amine, carboxylic acid or sulfonic acid, aryl ring, and hetero-atom hydrogen bonding moieties) which can potentially approximate the basic and acidic

groups of L-glutamate. In the instance of the dyes however, a direct correspondence of the positioning of these substitutions and the functional groups of L-glutamate is even less straight-forward than was previously modeled for the kynurenic acid analogues (Chapter 3).

A structural characteristic of this class of dyes not present in the kynurenic acid analogues is the inclusion of one or two aromatic side chains linked to the bicyclic core via a diazo bond. Although the role of these diazo-linked groups in binding to the transporter is as yet unknown, it is possible that they may be directly involved or, alternatively, may affect the chemical characteristics of the adjacent functional groups (e.g. pKa of amine or hydroxy moiety).

Similar to kynurenic acid, some of these dyes have been reported to interact with other components of the glutamatergic system. Evans Blue, for example, has been shown to non-competitively inhibit glutamate-evoked currents mediated by EAA ionotropic receptor subtypes in transfected HEK 293 cells (Price and Raymond, 1996) and in *X. laevis* oocytes (Keller et al., 1993). This inhibition appears to be limited to the AMPA and KA type receptors, although it is disputed whether this dye selectively binds to one subtype over the other. Interestingly, little if any inhibition of AMPA or KA receptor binding was observed with the structurally related dyes Chicago Sky Blue and Congo Red (Keller et al., 1993).

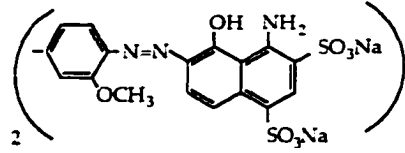
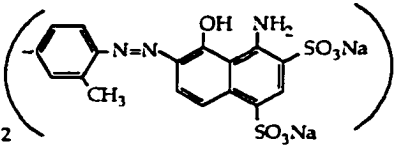
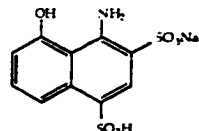
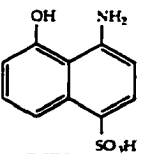
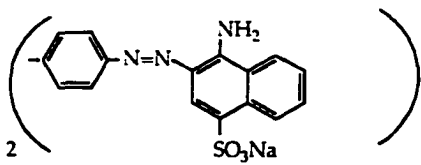
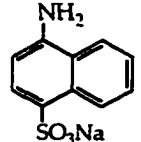
In this chapter, the inhibitory properties of these naphthylamine disulfonic acid dyes on the vesicular glutamate transporter are further characterized. A library of closely related compounds was chosen to study the structure-activity relationships and kinetic properties which governed their interactions with the vesicular uptake system. In particular, the contribution of the aromatic side chains to the inhibitory activity of the dyes was addressed by comparing analogous naphthalene sulfonic acids with and without the diazo-linked substituents. In addition, the relative positions of specific functional groups around the naphthalene carbon ring framework was examined. As a consequence of this work, several naphthalene sulfonic acid dyes have been identified which potently inhibit the uptake of $^3\text{H-L}$ -glutamate into synaptic vesicles. Parallel studies determined the cross-reactivities of these compounds with the high-affinity sodium-dependent synaptosomal glutamate transporter and with the EAA ionotropic receptors. These findings help to further refine our knowledge of the vesicular glutamate pharmacophore and identify new probes with which to explore its function.

Results

Synaptic vesicle transporter pharmacology: inhibition by naphthalene sulfonic acid dyes

These series of naphthalene sulfonic acids were initially tested at a single concentration (5 mM) for their ability to inhibit the uptake of $^3\text{H-L}$ -glutamate (0.25 mM) into synaptic vesicles isolated from rat forebrain (Tables 4.1 and 4.2). The concentration dependence of the inhibitory activity was then determined for those compounds exhibiting marked activities in the initial pharmacological assays (Figure 4.1, Table 4.3). As anticipated, the dyes Evans Blue and Chicago Sky Blue reduced the uptake of $^3\text{H-L}$ -glutamate into synaptic vesicles to background levels (Fyske et al., 1992). Control transport values were 3.83 ± 0.39 nmol/min/mg protein (Table 4.1). Indeed these two dyes were among the most potent inhibitors identified in this study, exhibiting similar K_i values of 0.21 ± 0.03 μM (i.e., determined from IC_{50} values according to the Cheng-Prusoff relationship; Cheng and Prusoff, 1973), Table 4.3. Almost equipotent with Evans Blue and Chicago Sky Blue, Naphthol Blue Black and Congo Red exhibited K_i values of 0.30 ± 0.12 and 0.49 ± 0.18 μM , respectively. A chemical characteristic common to these four dyes is the inclusion of two diazo linked aromatic side chains within their structures. In contrast, dyes containing only one diazo linked aromatic side

Table 4.1 Inhibition of ^3H -L-glutamate uptake into synaptic vesicles by naphthalene sulfonic acids

Compound	Structure	Vesicular Uptake of ^3H -L-Glutamate (% of Control)
<i>Chicago Sky Blue Analogues</i>		
Chicago Sky Blue		0 ± 0 (4)
Evans Blue		0 ± 0 (3)
1-Amino-8-naphthol-2,4-disulfonic acid (Chicago Acid)		2.9 ± 0.8 (3)
4-Amino-5-hydroxy-1-naphthalene sulfonic acid		3.8 ± 1.5 (6)
<i>Congo Red Analogues</i>		
Congo Red		1.4 ± 0.7 (3)
4-amino-1-naphthalene sulfonic acid		54.5 ± 5.9 (5)

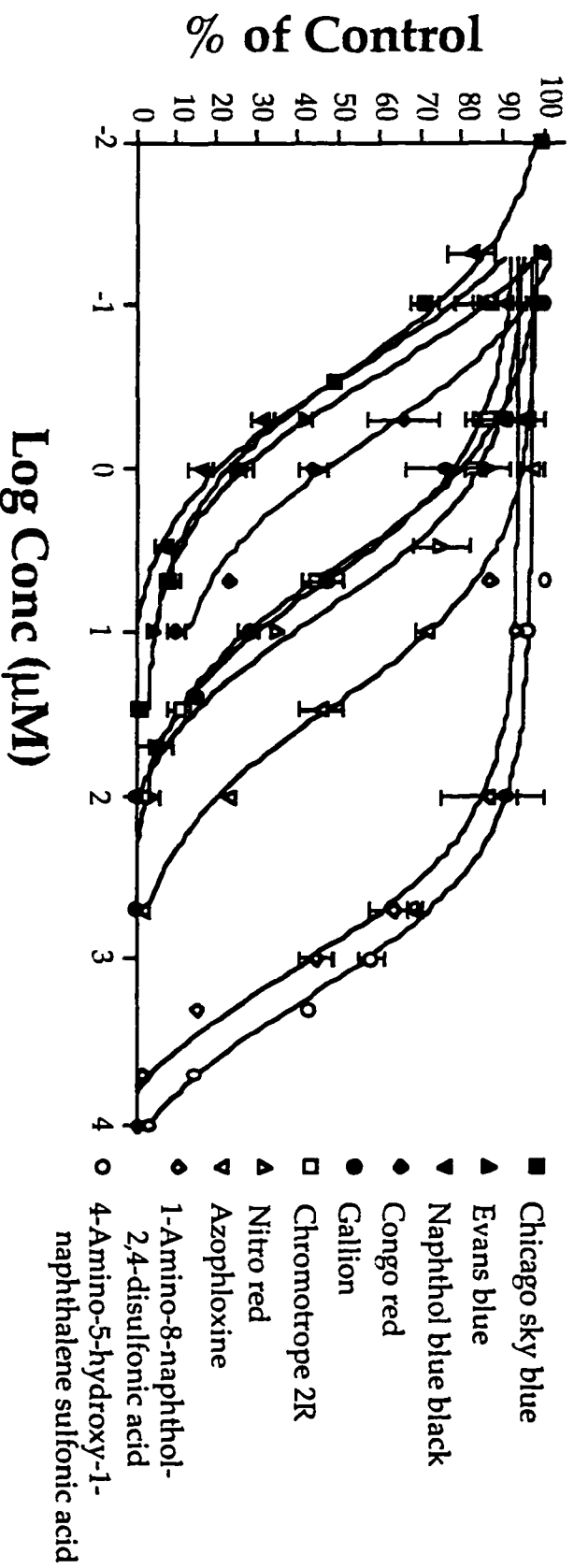
The vesicular uptake of ^3H -L-glutamate (0.25 mM) was performed as described in Chapter 2. Naphthalene sulfonic acids were present in the incubation medium at a final concentration of 5 mM. Results are reported as a percentage of control uptake \pm SEM with n number of experiments in parentheses. The control value for glutamate uptake was 3.83 ± 0.39 nmol/min/mg protein ($n = 14$).

Table 4.2 Inhibition of ^3H -L-glutamate uptake into synaptic vesicles by naphthalene sulfonic acids

Compound	Structure	Vesicular Uptake of ^3H -L-Glutamate (% of Control)
<i>Naphthol blue black analogues</i>		
Naphthol Blue Black		0.8 ± 0.8 (3)
Gallion		0 ± 0 (3)
Nitro Red		0.2 ± 0.2 (3)
Azophloxine		1.0 ± 0.4 (3)
Chromotrope 2R		0 ± 0 (3)
4-Amino-5-hydroxy-2,7-naphthalene disulfonic acid		30.9 ± 3.3 (5)
1-Naphthol-3,6-disulfonic acid		44.7 ± 3.3 (3)

The vesicular uptake of ^3H -L-glutamate (0.25 mM) was performed as described in Chapter 2. Naphthalene sulfonic acids were present in the incubation medium at a final concentration of 5 mM. Results are reported as a percentage of control uptake \pm SEM with n number of experiments in parentheses. The control value for glutamate uptake was 4.35 ± 0.41 nmol/min/mg protein ($n = 9$).

41 Figure 4.1 Demonstration of the inhibitory dose-response dependency of naphthalene sulfonic acids on ³H-L-glutamate uptake into synaptic vesicles.



The uptake of ³H-L-glutamate (0.25 mM) was performed as described in Chapter 2. Naphthalene sulfonic acids were included in the assays over a range of concentrations. Individual graph data points represent the mean percentage of control \pm SEM for 3-4 experiments. The control value for glutamate uptake was 3.34 ± 0.27 nmol/min/mg protein ($n = 14$).

Table 4.3 Inhibitory potencies of naphthalene sulfonic acids on vesicular ^3H -L-glutamate uptake.

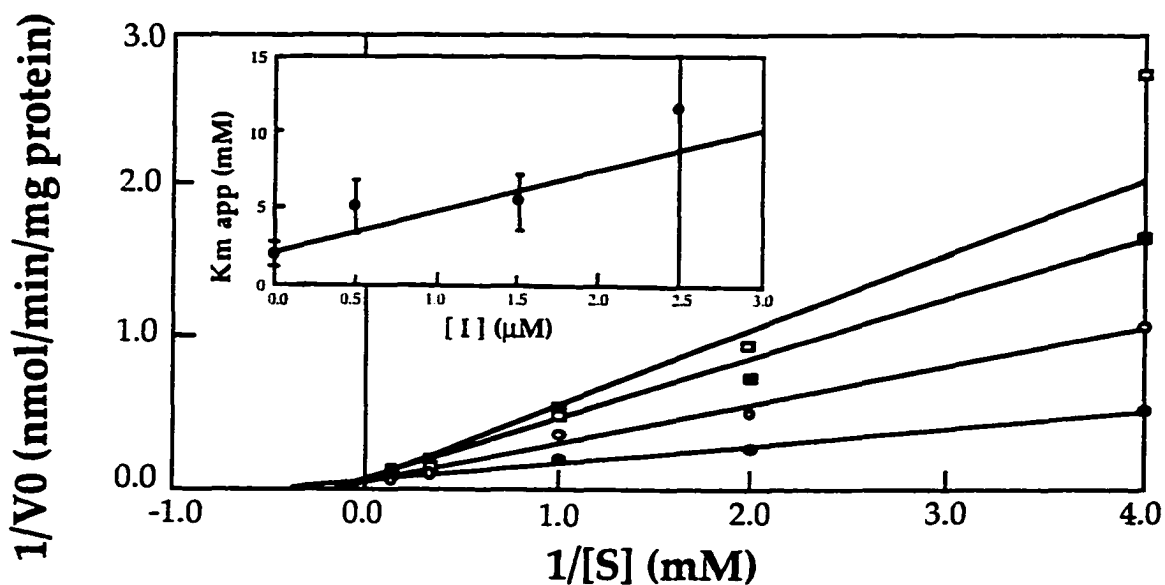
Compound	IC_{50} (μM)	K_i (μM)
Chicago sky blue	0.24 ± 0.04 (3)	0.21 ± 0.03 (3)
Evans blue	0.23 ± 0.03 (4)	0.21 ± 0.03 (4)
Naphthol blue black	0.34 ± 0.12 (3)	0.30 ± 0.12 (3)
Congo red	0.55 ± 0.20 (4)	0.49 ± 0.18 (4)
Gallion	3.90 ± 0.94 (4)	3.47 ± 0.83 (4)
Chromotrope 2R	5.53 ± 1.27 (3)	4.91 ± 1.13 (3)
Nitro red	6.95 ± 1.92 (3)	6.18 ± 1.71 (3)
Azophloxine	32.56 ± 4.21 (3)	28.9 ± 3.74 (3)
1-Amino-8-naphthol-2,4-disulfonic acid	1058 ± 330 (3)	940 ± 294 (3)
4-Amino-5-hydroxy-1-naphthalene sulfonic acid	2424 ± 376 (3)	2155 ± 334 (3)

The transport of ^3H -L-glutamate (0.25 mM) into synaptic vesicles was performed as described in Chapter 2. IC_{50} values were determined from non-linear regression analyses according to a one-site competition model. K_i values were estimated from IC_{50} values according to the Cheng-Prusoff relationship. Results are reported as mean \pm SEM with n number of experiments in parentheses.

chain (e.g. Gallion, Chromotrope 2R, Nitro Red, and Azophloxine) proved to be at least an order of magnitude less potent as inhibitors of vesicular ^3H -L-glutamate uptake (e.g. K_i values ranging from 3.47 - 28.9 μM). It must be taken into consideration, however, that these compounds still exhibited a 50 - 1000 fold greater ability to inhibit vesicular uptake than the endogenous substrate L-glutamate.

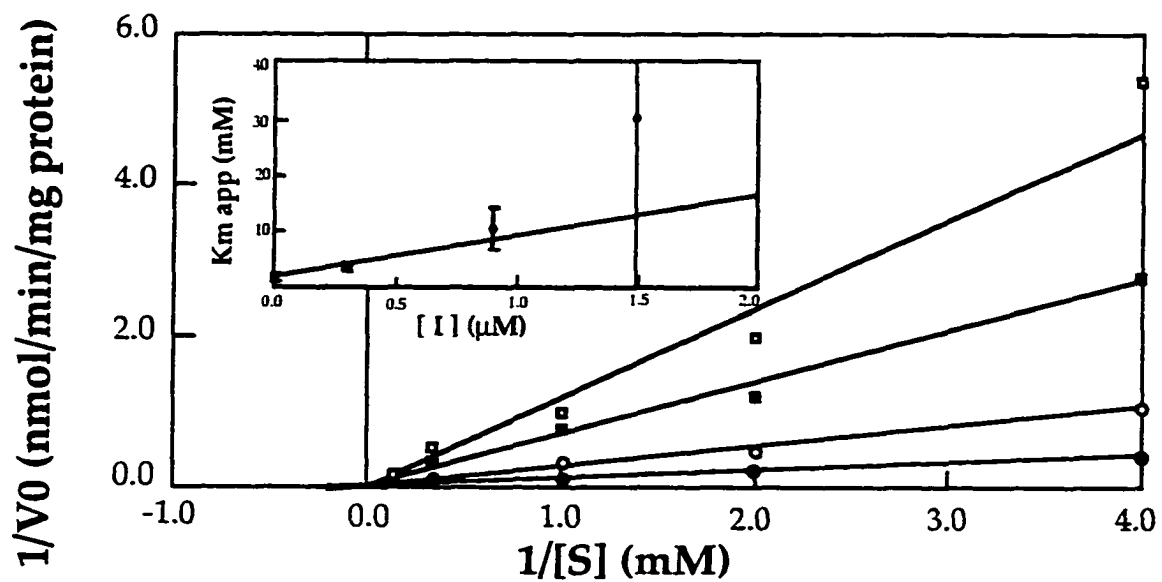
To confirm the competitive nature of this inhibition by the naphthylamine sulfonic acid dyes, more detailed kinetic analyses were carried out with two of the most potent inhibitors. Representative Lineweaver-Burk plots are illustrated for the inhibition of vesicular glutamate uptake by Congo Red and Naphthol Blue Black in Figures 4.2 and 4.3, respectively. The K_m and V_{max} values for the transport of L-glutamate were found to be 1.87 ± 0.12 mM and 18.26 ± 1.26 nmol/min/mg protein ($n = 7$). Similar to the previous findings for Evans Blue and Chicago Sky Blue, the patterns of inhibition exhibited by Congo Red and Naphthol Blue Black were consistent with the actions of competitive inhibitors. K_i values were determined on the basis of a replot of K_m apparent values (insets Figures 4.2 and 4.3) *versus* inhibitor concentrations and were found to be 0.70 ± 0.25 for Congo Red and 0.37 ± 0.11 μM for Naphthol Blue Black. In both instances, these values were comparable to those determined from IC_{50} values and the Cheng-Prusoff calculations as reported in Table 4.3.

Figure 4.2 Demonstration of the competitive inhibition by Congo Red on ^3H -L-glutamate uptake into synaptic vesicles.



Representative Lineweaver-Burk plot of a single experiment demonstrating competitive inhibition by Congo Red (0.5, 1.5, 2.5 μM) on the uptake of ^3H -L-glutamate (0.25 - 8.0 mM) into rat brain synaptic vesicles. The above plots yielded a control $V_{max} = 17.94 \pm 3.39$ nmol/min/mg protein and $K_m = 2.06 \pm 0.59$ mM. Inset shows a replot of K_m apparent versus Congo Red concentration producing a $K_i = 0.84 \pm 0.34$ μM .

Figure 4.3 Demonstration of the competitive inhibition by Naphthol Blue Black on ^3H -L-glutamate uptake into synaptic vesicles.



Representative Lineweaver-Burk plot of a single experiment demonstrating competitive inhibition by Naphthol Blue Black (0.3, 0.9, 1.5 μM) on the uptake of ^3H -L-glutamate (0.25 - 8.0 mM) into rat brain synaptic vesicles. The above plots yielded a control $V_{max} = 17.15 \pm 0.36$ nmol/min/mg protein and $K_m = 1.64 \pm 0.06$ mM. Inset shows a replot of K_m apparent *versus* Naphthol Blue Black concentration producing a $K_i = 0.22 \pm 0.03$ μM .

The significance of the diazo-linked groups of these naphthalene sulfonic acid dyes was evaluated by comparing several compounds which lacked the aromatic side chains, yet contained the same core structural frameworks (i.e., naphthalene ring with the analogous functional group substitutions). The two such compounds that possess the same core structure as Evans Blue and Chicago Sky Blue, 1-amino-8-naphthol-2,4-disulfonic acid and 4-amino-5-hydroxy-1-naphthalene sulfonic acid, reduced ^3H -L-glutamate uptake by the synaptic vesicles to 2.9 and 3.8 % of Control, respectively (Table 4.1). Further investigation revealed that the K_i values exhibited by these compounds (940 ± 294 and $2155 \pm 334 \mu\text{M}$, respectively, Table 4.3) were more on par with those of L-glutamate and kynurenate (see Chapter 3), rather than those of the parent compounds. Similarly, the analogous core compound of Naphthol Blue Black, 4-amino-5-hydroxy-2,7-naphthalene disulfonic acid, reduced vesicular ^3H -L-glutamate uptake to only 30.9 % of Control (Table 4.2). Clearly, the diazo-linked aromatic side chains of these dyes play an important role in increasing the affinity with which these compounds bind to the vesicular transporter.

Pharmacological specificity of naphthalene sulfonic acids

The potential cross-specificities of the naphthalene sulfonic acids with other components of the glutamatergic system, was in part assessed by examining the ability of these compounds to block the sodium-dependent uptake of ^3H -D-aspartate into synaptosomes and radioligand binding to EAA ionotropic receptors on rat forebrain synaptic plasma membrane (see Chapter 2). As reported in Table 4.4, Evans Blue and Congo Red were found to be the most potent inhibitors of synaptosomal transport, reducing the uptake of ^3H -D-aspartate (5 μM) to 4.1 and 6.5% of Control (1.10 ± 0.04 nmol/min/mg protein) respectively, when included in the assays at a concentration of 250 μM . Chicago Sky Blue and Naphthol Blue Black reduced the uptake to approximately 50% of Control and only moderate levels of inhibition were observed with the other compounds.

These naphthalene sulfonic acids were then examined for their ability to block the binding of ^3H -L-glutamate (10 nM) to NMDA receptors, ^3H -kainate (10 nM) to kainate receptors, and ^3H -AMPA (10 nM) to AMPA receptors (Table 4.5). The results are reported as percentages of Control: 0.13 ± 0.01 pmol/mg protein for ^3H -L-glutamate, 0.22 ± 0.03 pmol/mg protein for ^3H -kainate, and 0.15 ± 0.02 pmol/mg protein for ^3H -AMPA. In agreement with previous studies (Price and Raymond, 1996; Keller et al., 1993), Evans Blue (100 μM) potently inhibited radioligand binding to the kainate and AMPA

Table 4.4 Inhibitory activities of naphthalene sulfonic acids on the uptake of $^3\text{H-D-aspartate}$ into rat forebrain synaptosomes.

Compound	Inhibition of Synaptosomal $^3\text{H-D-Aspartate}$ Uptake (% of Control)	
	Concentration (250 μM)	Concentration (25 μM)
Chicago Sky Blue	51.5 \pm 3.3 (3)	80.9 \pm 4.8 (7)
Evans Blue	4.1 \pm 0.5 (3)	38.9 \pm 3.4 (7)
Naphthol Blue Black	46.9 \pm 3.3 (3)	80.4 \pm 4.2 (7)
Congo Red	6.5 \pm 3.2 (3)	36.5 \pm 3.1 (7)
1-Amino-8-naphthol- 2,4-disulfonic acid	78.5 \pm 11.2 (3)	
4-Amino-5-hydroxy-1- naphthalene sulfonic acid	74.7 \pm 18.0 (3)	
Gallion	73.0 \pm 10.9 (3)	
Nitro Red	85.1 \pm 7.6 (3)	
Azophloxine	82.5 \pm 3.3 (3)	
Chromotrope 2R	70.4 \pm 1.3 (3)	

The abilities of the compounds listed above to block the uptake of $^3\text{H-D-aspartate}$ (5 μM) into rat forebrain synaptosomes was determined as described in Chapter 2. Results are reported as the mean \pm SEM of the percentage of control uptake (1.10 \pm 0.04 nmol/min/mg protein) with n number of experiments in parentheses.

Table 4.5 Pharmacological specificity of naphthalene sulfonic acids as inhibitors of EAA ionotropic receptor binding.

Compound	³ H-L-GLU binding to NMDA receptors (% of Control)	³ H-AMPA binding to AMPA receptors (% of Control)	³ H-KA binding to KA receptors (% of Control)
Chicago Sky Blue	4.5 ± 2.5 (9)	42.1 ± 4.4 (10)	12.7 ± 3.2 (6)
Evans Blue	< 0 (4)	52.3 ± 6.4 (5)	40.5 ± 5.9 (3)
Naphthol Blue Black	69.5 ± 7.6 (5)	92.1 ± 6.7 (5)	90.4 ± 3.9 (3)
Congo Red	1.4 ± 1.6 (6)	48.6 ± 3.5 (11)	15.2 ± 6.0(6)
Gallion	67.7 ± 8.8 (9)	77.0 ± 5.5 (9)	65.4 ± 2.6 (5)
Chromotrope 2R	95.1 ± 3.5 (6)	101.5 ± 3.4 (3)	91.5 ± 5.9 (4)
Nitro Red	92.2 ± 8.3 (6)	93.2 ± 3.9 (6)	81.5 ± 4.7 (4)
Azophloxine	107.8 ± 2.8 (4)	105.4 ± 2.1 (5)	95.3 ± 5.3 (4)
1-Amino-8-naphthol-2,4-disulfonic acid (Chicago acid)	35.4 ± 6.4 (9)	72.2 ± 2.5 (8)	66.6 ± 6.9 (5)
4-Amino-5-hydroxy-1-naphthalene sulfonic acid	73.5 ± 12.7 (5)	96.1 ± 4.3 (5)	60.2 ± 6.2 (4)
4-Amino-5-hydroxy-2,7-naphthalene disulfonic acid	90.5 ± 13.0 (6)	98.8 ± 4.5 (5)	75.8 ± 7.4 (4)
4-Amino-1-naphthalene sulfonic acid	100.6 ± 7.6 (5)	109.5 ± 8.0 (5)	95.4 ± 8.9 (4)

EAA ionotropic receptor binding was selectively assayed as described in Chapter 2. Naphthalene sulfonic acids were included in the assays at a concentration of 100 μM. All values represent specific binding and are reported as the means of the percentage of control binding ± SEM, with *n* number of experiments in parentheses.

receptors reducing levels to 40.5 and 52.3 % of Control, respectively. Its inhibitory activity was even more substantial at the NMDA receptor, where the amount of binding was reduced to background levels. Similarly, Chicago Sky Blue and Congo Red exhibited a marked affinity for each of these EAA receptors. In contrast, the naphthylamine dyes with 3,6-disulfonic acid substitutions exhibited much less cross-specificity with the EAA receptors. For instance, Chromotrope 2R, Nitro Red, and Azophloxine caused very little if any inhibition of radioligand binding. Naphthol Blue Black reduced binding to the NMDA receptor to only 69.5% of Control and had virtually no effect on AMPA and KA receptor binding.

Discussion

In this study, several naphthylamine sulfonic acid dyes have been identified as potent inhibitors of the glutamate transporter on synaptic vesicles. Of these, Evans Blue, Chicago Sky Blue, Naphthol Blue Black, and Congo Red were determined to be the most potent with K_i values ranging from about 0.2 to 0.5 μM (Figure 4.3). Lineweaver-Burk kinetic analyses demonstrate that the nature of this inhibition is competitive and indicates that these compounds have greater than a 4000-fold higher apparent affinity for the transporter binding site than the endogenous substrate L-glutamate

($K_m \approx 2 \text{ mM}$). Since this interaction with the transporter is competitive, it would seem plausible to expect that these dyes bind in an analogous fashion to that of L-glutamate. Yet, comparison between the chemical structures of these compounds and L-glutamate is even less straight-forward than what was previously proposed for the kynurenic acid analogues in Chapter 3. In addition, key structural differences exist between these four dyes (e.g. placement of functional groups around the naphthalene ring system), which belie the similar levels of inhibitory activity exhibited toward vesicular glutamate uptake. In light of these findings, it is likely that these compounds may interact with the vesicular transporter in a manner different than that of L-glutamate.

Clearly, a comparison between the functional groups of the compounds listed in Tables 4.1 and 4.2, suggests that there is a great deal of flexibility in the regio-positioning of the groups around the naphthalene ring system. For example, among the most potent dyes (e.g. Evans Blue, Chicago Sky Blue, Naphthol Blue Black, and Congo Red), the sulfonic acids may occupy positions 2,4-, 3,6-, or 4- in relation to the exocyclic amine and still retain activity. Additionally, location of the hydroxy and amine moieties at positions 1- and 8- appear to be interchangeable or not required. This condition is best demonstrated among the compounds Gallion, Nitro red, and Chromotrope 2R where these functional groups are interchanged relative to the position of the diazo-linked aromatic side chain, and a similar level of

activity is retained ($K_i = 3.47$ to $6.18 \mu\text{M}$). Interestingly though, about a 6 fold reduction in activity is observed with Azophloxine (relative to Chromotrope 2R) which incorporates an acetylated amine at position 1-. This difference may reflect steric effects caused by this bulky substitution with the transporter protein.

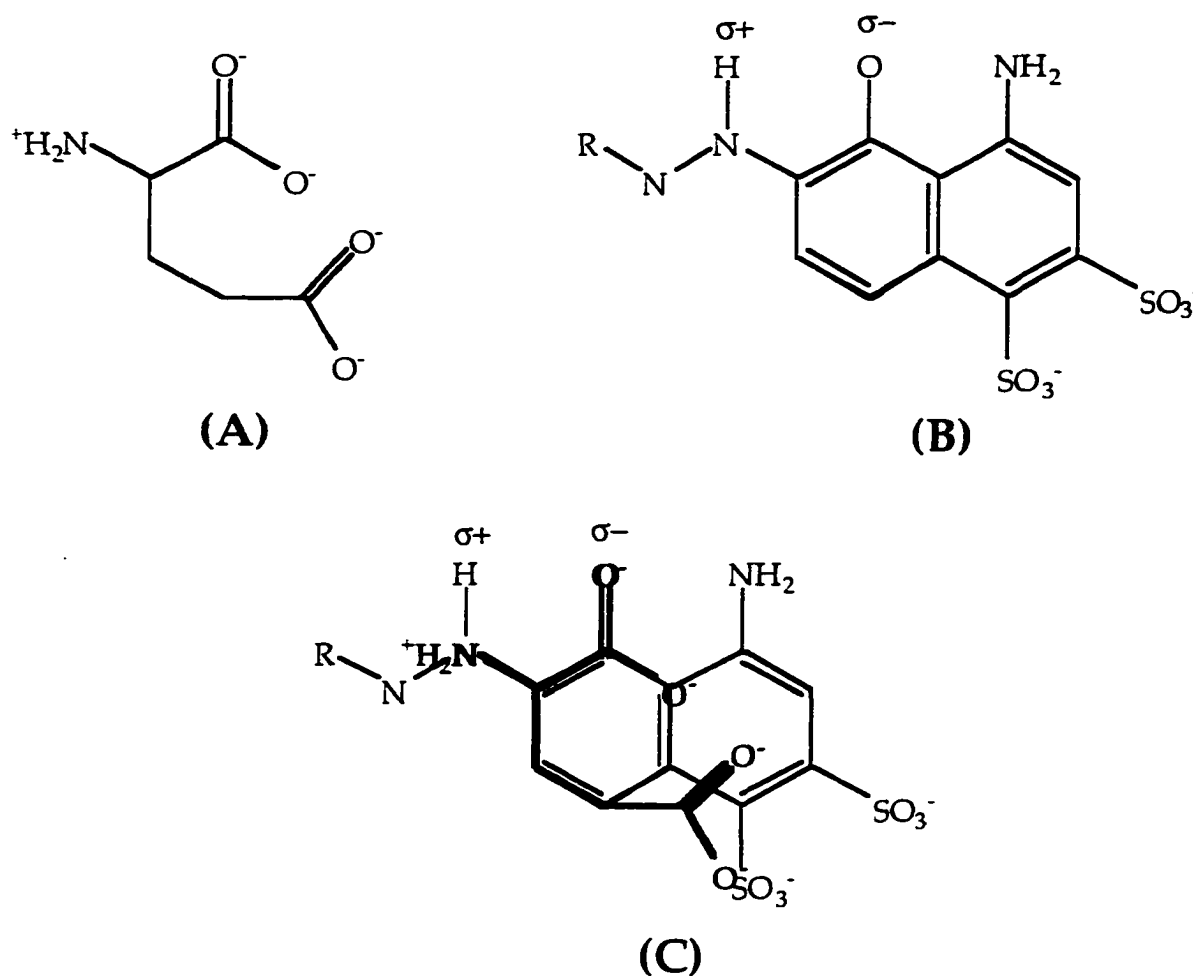
An even more dramatic reduction in inhibitory activity is observed when the diazo-linked aromatic side chain is removed. As seen with the core bicyclic frameworks of these dyes, Chicago acid and 4-amino-5-hydroxy-2,7-naphthalene disulfonic acid, a ≥ 4700 fold reduction in inhibitory activity occurs when the diazo-linked groups are absent. A similar conclusion was reached in a recent study where the core substituted naphthylamine sulfonic acids elicited no inhibitory activity on vesicular glutamate transport when compared to the activities of the analogous parent dye molecules (Roseth et al., 1998).

There are several possible explanations for the increased activity of the dyes containing diazo-linked aromatic side chains. First, the diazo linkage may play a direct role in binding to the transporter or may affect the chemical characteristics of adjacent functional groups. Since the diazo group nitrogens are electron rich, they may act to withdraw a proton from the adjacent amino or hydroxy functional group thereby generating a hydrogen bonding capacity. Consequently, the diazo group would carry a partial charge from this interaction and in combination with the adjacent hydrogen bonding group

may approximate the α -amino and α -carboxy groups of L-glutamate. The γ -carboxylate group of L-glutamate in this paradigm could be approximated by the substituted 3- or 4- sulfonic acid substituent (Figure 4.4). Second, the aromatic substituent attached via the diazo-linkage may interact with a complimentary hydrophobic pocket on or near the substrate binding site of the transporter protein. For this reason, exactly mimicking the conformation with which glutamate binds to the vesicular transporter may not be required in order to achieve maximum inhibitory activity. In fact, if this hypothesized hydrophobic interaction is valid, pursuing inhibitors of this class rather than the more obvious glutamate analogues may prove to be more beneficial, as they are at least 1000 fold greater in potency than glutamate itself and may exhibit less cross-reactivity with other components of the EAA system. Third, the addition of the diazo-linked side chain may serve to effectively elongate the molecule and interfere with a conformational change in the transporter after binding of the inhibitor. Since the primary function of the transporter is to bind and translocate a substrate across the vesicular membrane, a conformational change in the protein is required to reorient the binding site from one surface of the membrane to the other. In regard to the dyes, transporter binding may be facilitated by the ionic substituents on the naphthalene ring, however, upon a subsequent conformational change in the protein, the presence of the diazo-linked side chain could prevent reorientation of the binding site across the membrane. Additionally, if the



Figure 4.4 Depiction of glutamate, naphthylamine sulfonic acid dyes, and an overlay of both showing the potential vesicular glutamate binding conformation.



Representative molecular line drawings depict (A) glutamate, (B) the core naphthylamine dye framework including sulfonic acids in the 3- and 4-positions (i.e. analogous to Naphthol Blue Black and Evans Blue respectively), and (C) a potential overlay aligning the α -nitrogen, α -carboxylate, and γ -carboxylate of glutamate with the diazo nitrogen, 8-hydroxy, and 4-sulfonic acid groups of the dye framework.

dyes initially stimulate the transport mechanism and then become trapped in the binding pocket due to a partial conformational change in the transporter, their apparent binding to the substrate site would be enhanced. Since the K_i value is a ratio of K_{on} and K_{off} rates (i.e., $K_i = K_{on}/K_{off}$), such an interaction would be observed as an increase in K_{off} and consequently a decrease in K_i .

Of these three possibilities, present evidence suggests that the latter two are the most likely. Recent studies have demonstrated that the addition of lipophilic groups appended to a quinoline 2,4-dicarboxylic acid framework at positions 6- or 7- also markedly increase inhibitory activity (unpublished data). Importantly, this enhanced activity is not dependent upon a diazo linkage to the quinoline ring system.

In conclusion, the present study demonstrates that among this naphthylamine sulfonic acid series of compounds, those linked via a diazo bond to an aromatic side chain exhibit the highest level of inhibitory activity at the vesicular glutamate transporter. The evidence suggests that this activity may be due to either a hydrophobic interaction with the transporter not required for substrate binding, or interference with the transporter mechanism. Since there appears to be a great deal of latitude in the positioning of ionic functional groups around the naphthalene ring system, an exact mimic of the L-glutamate conformer which binds to the transporter may not be preferred for optimal inhibitory activity. In fact, since little cross-reactivity was observed with many of the 3,6- disulfonic acid substituted dyes

at other EAA sites, these may be ideal lead compounds for the development of more potent and selective inhibitors of this transport system. As inhibitors emerge with increasing potency and specificity, they shall prove invaluable as probes of vesicular glutamate transport.

Chapter 5: Characterization of the vesicular transporter mechanism: Roles of ATP-dependence, trans-stimulation, and efflux attenuation.

Introduction

Early investigations focused on characterizing the action of glutamate as an excitatory transmitter, and demonstrated that subcellular fractions of synaptic vesicles contain relatively low levels of this amino acid following their isolation by variable speed centrifugation and gel filtration (De Belleruche and Bradford, 1973). Since the synaptic vesicles were not found to be substantially enriched with glutamate, it raised the possibility that during neuronal firing this amino acid may be released from cytosolic rather than vesicular stores. This issue was later resolved using TEM and immunocytochemical labeling for L-glutamate, when studies demonstrated that high levels of glutamate are present in the synaptic vesicles of specific nerve endings (Storm-Mathisen et al., 1983). Consistent with this conclusion, numerous studies have shown that isolated synaptic vesicles rapidly accumulate glutamate and that this uptake is dependent upon the presence of an electrochemical proton gradient generated by a vacuolar-type Mg^{++} -ATPase (Naito and Ueda, 1983; Naito and Ueda, 1985; Maycox et al., 1988). In this

regard, it is likely that the electrochemical gradient required for glutamate uptake, is also required for glutamate retention by synaptic vesicles. Thus, in retrospect, if the proton gradient was not maintained during previous isolation attempts, it would explain the lack of glutamate present within the vesicle fraction. That this was indeed occurring, was later verified by Burger et al., (1989), when it was demonstrated that glutamate efflux during synaptic vesicle isolation could be attenuated by the inclusion of ATP in the isolation medium. Further the treatment of synaptic vesicles with N-ethylmaleimide (NEM), could also attenuate the efflux, presumably by modifying a sulfhydryl moiety required for transporter function.

In addition to the dependence upon a proton gradient, the vesicular transporter is also affected by the concentration gradient of L-glutamate between the vesicle lumen and the extravesicular environment. Studies have demonstrated that by diluting synaptic vesicles containing $^3\text{H-L}$ -glutamate into a buffer in which concentrations of substrates are reduced to a level at which uptake is negligible, a rapid efflux of the vesicle contents is observed (Carlson and Ueda, 1990; Wang and Floor, 1994). Further, this efflux was hypothesized to be carrier-mediated since it was found to be attenuated by both reduced temperature and treatment with NEM. These findings support the conclusion that transport through the vesicle carrier is bi-directional and raises an interesting question regarding this transport mechanism. Since glutamate efflux is apparently mediated by a reversal of the transport process,

can the rate of efflux out of the vesicle be increased by the addition of external substrate? This process, referred to as *trans*-stimulation, has been observed with a number of transport systems (Christensen, 1975). It was previously reported that the rate of vesicular ^3H -dopamine efflux could be increased over control levels when unlabeled dopamine was included in the dilution medium (Floor et al., 1995). This same study also demonstrated that the inclusion of a non-transportable inhibitor, reserpine or tetrabenazine, decreased the rate of ^3H -dopamine efflux below that of Control levels. Presumably, this effect is due to the extravesicular occupation of the transporter substrate binding site by the inhibitor, causing a decrease in ^3H -dopamine efflux by favoring the orientation of the transporter towards the extravesicular surface.

In this chapter, two aspects of the process of vesicular glutamate transport are examined in greater detail. First, the role of ATP in establishing and maintaining glutamate concentrations within synaptic vesicles is addressed. Second, the effect of the application of the inhibitors previously identified in Chapters 3 and 4 on this vesicular glutamate pool is examined. Through the latter studies, a potential paradigm is presented for the rapid identification and differentiation of substrates *versus* non-substrates by determining the abilities of these compounds to either initiate the *trans*-stimulation of vesicular glutamate (substrate) or block its efflux (non-substrate) from synaptic vesicles. Therefore, the utility of these compounds

extends beyond their use in specificity studies, as they can be additionally used to probe the mechanism of transporter function.

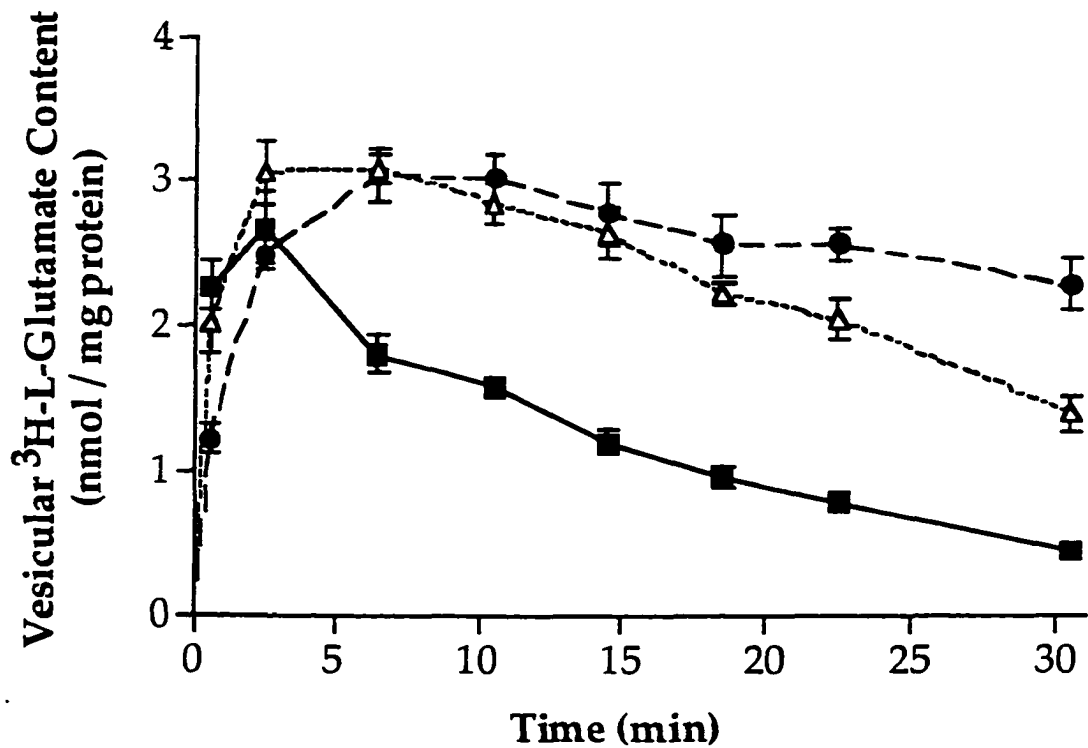
Results

ATP-dependence of ³H-L-glutamate uptake and retention

Initial studies attempted to isolate synaptic vesicles containing accumulated ³H-L-glutamate by differential centrifugation (222,000 × g_{max} , 55 min) in the presence of 2 mM ATP. Following the centrifugation however, less than 30% of the original ³H-L-glutamate remained in the vesicle fraction (data not shown). It was assumed that this loss was most likely attributable to the consumption of ATP during the re-isolation phase, and consequently a reduction in the electrochemical proton gradient generated by the vesicular Mg⁺⁺-ATPase. This could have resulted in an efflux of glutamate from the synaptic vesicles, since a disruption of the proton gradient has been previously linked with a decrease in ³H-L-glutamate uptake (Naito and Ueda, 1983; Naito and Ueda, 1985; Maycox et al., 1988). In order to test this hypothesis, experiments were conducted in which the concentration of ATP in the uptake assays was varied from 2-6 mM. The incubations were carried out for a period of 30 min and at the indicated times, aliquots were removed

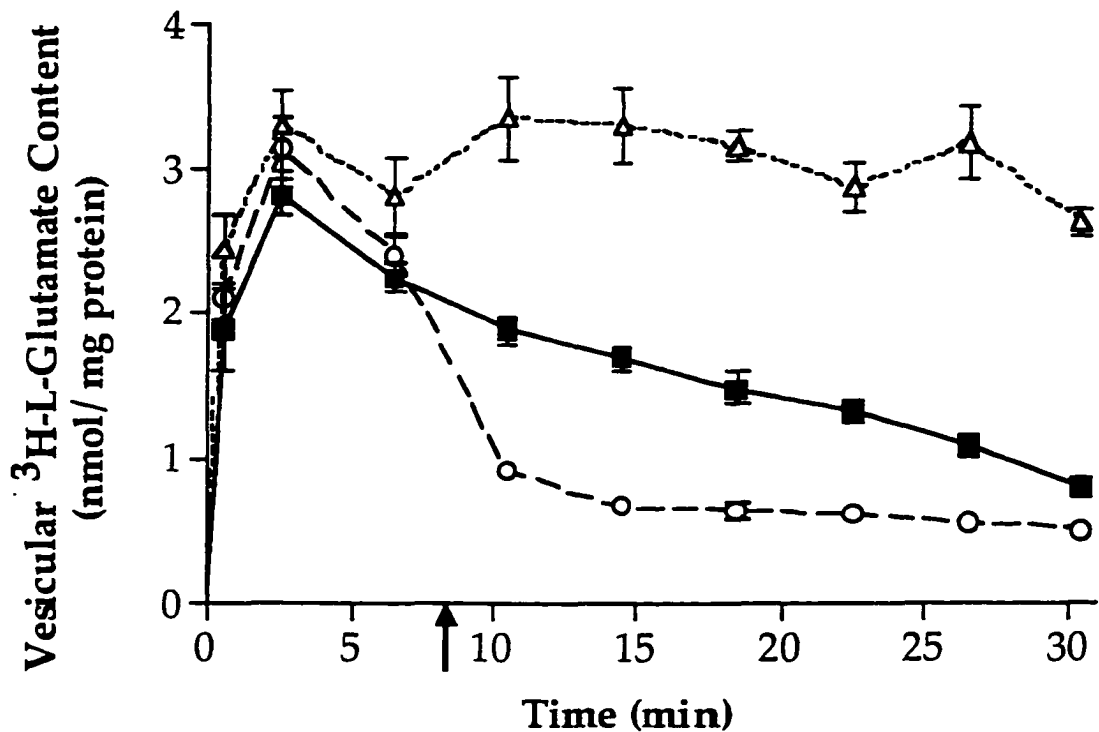
to monitor glutamate levels within the vesicle fraction of the individual assays. Due to the small size of the aliquots (25 μ L), vesicle protein content in the incubations was increased 4-5 fold relative to the standard transport assay to obtain a measurable signal. As shown in Figure 5.1, in the presence of 2 mM ATP, there was a rapid accumulation of glutamate by the synaptic vesicles that reached near maximum levels (2.5 - 3.5 nmol/mg protein) in 2-3 min. This was followed shortly thereafter by efflux of the radiolabel to almost background levels. When the ATP concentration was increased to 4 mM, a similar maximal level was reached, but in this case the intracellular level was maintained for up to 15 min. The length of time for which this maximal level of glutamate was sustained increased to almost 30 min when the ATP level was increased to 6 mM. These results suggest that not only is ATP required for the initial sequestration of glutamate by synaptic vesicles, but also for its maintenance in the vesicle lumen. This conclusion is further supported by a second set of experiments in which ATP was re-added during the incubation. As shown in Figure 5.2, the addition of a second aliquot of ATP (at an assay equivalent of 3 mM) at 8 min prevented the previously observed efflux and allowed the amount of glutamate accumulated by the synaptic vesicles to be maintained over the 30 min incubation period. In contrast, the addition of carbonyl cyanide p-trifluoromethoxyphenylhydrazone (FCCP, 1 μ g/ml) at 8 min caused the immediate efflux of accumulated glutamate. Consistent with previous

Figure 5.1 ATP dependence of vesicular $^3\text{H-L-glutamate}$ accumulation and retention



$^3\text{H-L-Glutamate}$ uptake into synaptic vesicles was measured in the presence of 2 mM ($\text{—}\blacksquare\text{—}$), 4 mM ($\text{---}\triangle\text{---}$), and 6 mM ATP ($\text{--}\bullet\text{--}$) as described in Chapter 2. Individual incubations were allowed to proceed for the indicated times before termination of uptake. Results represent the mean \pm SEM for $n = 4$ determinations.

Figure 5.2 Dependence of vesicular $^3\text{H-L-glutamate}$ retention on ATP



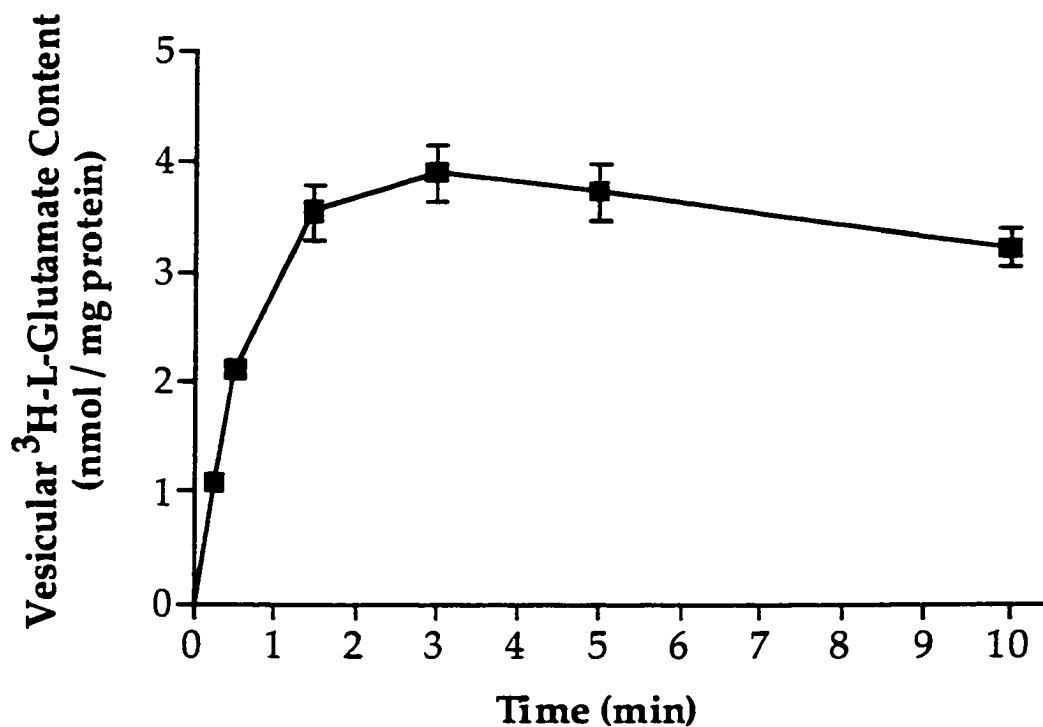
Vesicular $^3\text{H-L-glutamate}$ uptake was carried out in the presence of 3 mM ATP essentially as described in Chapter 2. The arrow represents a 5 μl addition at 8 min yielding a final assay concentration of: 3 mM ATP (--- Δ ---), ethanol, (— \blacksquare —), 1 $\mu\text{g/ml}$ FCCP in ethanol (--- \circ ---). Individual incubations were allowed to proceed for the indicated times before termination of uptake. Results represent mean \pm SEM for $n = 4$ determinations.

findings (Carlson and Ueda, 1990; Maycox et al., 1988), the rapid efflux caused by this ionophore is likely due to an abolished proton gradient. Since this effect is not attributed to an inhibition of the Mg^{++} -ATPase, it is independent of the ATP concentration.

Glutamate induced trans-stimulation

While the experiments described in the previous section demonstrate that disruption of the proton gradient, either by energy depletion or the addition of an ionophore, results in the efflux of glutamate from synaptic vesicles, they fail to address the route of this efflux. This raises questions as to whether or not this transport process is bi-directional and if the efflux of L-glutamate occurs through the same carrier responsible for its uptake *via* the reversal of the transport process. To address this question an approach was required that permitted the rate of vesicular glutamate efflux to be easily quantified under various experimental conditions. First, it was necessary to determine the stability of the accumulated vesicular glutamate pool under the assay conditions described in Chapter 2 (2 mM ATP, 0.25 mM 3H -L-glutamate, 100-150 μ g vesicle protein content, etc.). As shown in Figure 5.3, maximum vesicular glutamate levels (\approx 4 nmol/mg protein) are reached within 3 min, and in general, maintained over the 10 min assay period. To

Figure 5.3 Time course for the ATP-dependent uptake of ^3H -L-glutamate into synaptic vesicles.



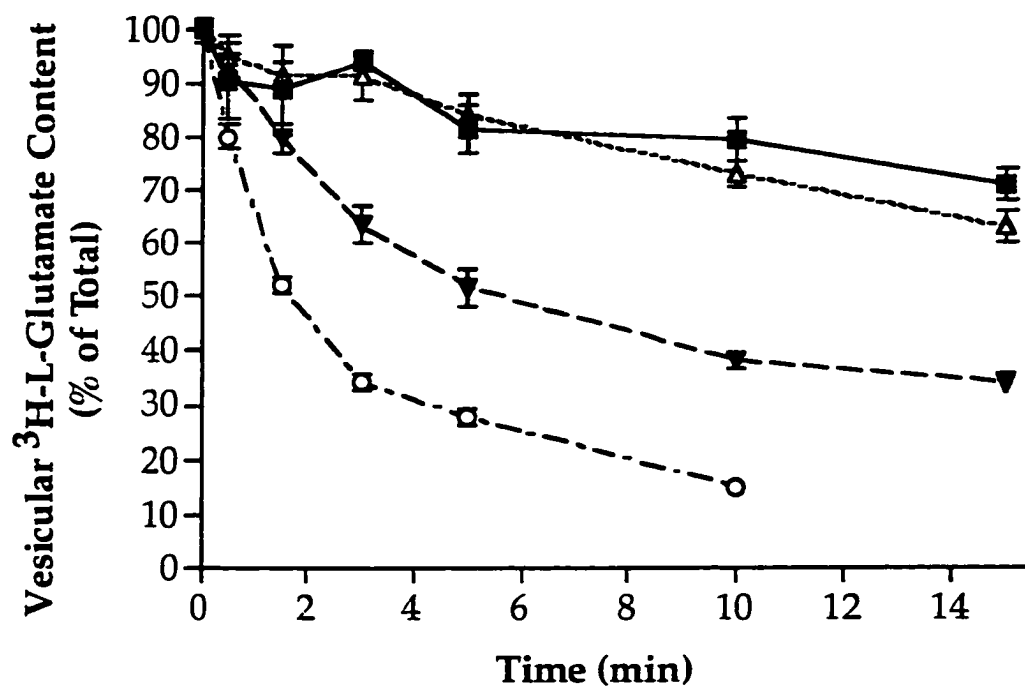
Vesicular ^3H -L-glutamate uptake was performed as described in Chapter 2 with termination of the assays at the times indicated. Values represent the mean \pm SEM for $n = 6$ determinations.

follow efflux, the vesicles were incubated under these conditions for 10 min, and then diluted 20 fold into buffer devoid of ATP and L-glutamate. In this manner the extravesicular levels of ATP and L-glutamate were decreased to at least 100 μM and 12.5 μM respectively. As illustrated in Figure 5.4, these dilutions resulted in the rapid efflux of ^3H -L-glutamate when the buffer was maintained at 30°C. Decreasing the temperature of the dilution buffer dramatically slowed this efflux process, as evidenced at 20, 10, and 2°C. The attenuation of glutamate efflux as a function of temperature is more consistent with a carrier mediated process rather than through an open channel or diffusion across the membrane, as these relatively small changes in temperature would not be expected to affect the latter processes.

The bi-directionality of vesicular transport raises a number of interesting possibilities. One addressed in the present work concerns whether or not efflux is affected by the presence of an external substrate. As illustrated in Figure 5.5, the inclusion of unlabeled L-glutamate in the dilution buffer at a concentration of 20 mM (i.e., 10x its K_m) significantly increases the initial rate of efflux. Such an increase is consistent with the process of *trans*-stimulation (for review see Christensen, 1975) and most likely reflects the exchange of internal for external substrate, rather than a net movement in any one direction.

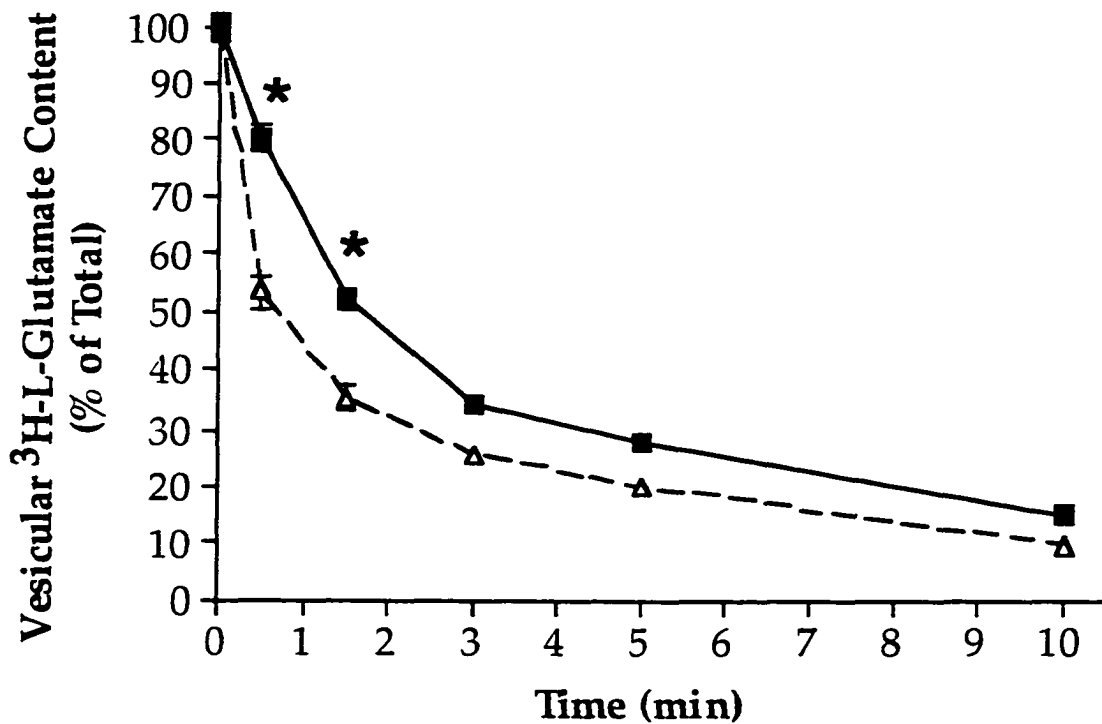
Advantageously, this exchange process can be employed to differentiate substrates from non-substrate inhibitors. At similar levels of occupancy of

Figure 5.4 Effect of temperature on $^3\text{H-L-glutamate}$ efflux from synaptic vesicles



The uptake of $^3\text{H-L-glutamate}$ was performed as described in Chapter 2. Following a 5 min incubation, assays were diluted 20 fold into buffers at 0°C ($\text{---}\blacksquare\text{---}$), 10°C ($\text{---}\blacktriangle\text{---}$), 20°C ($\text{---}\blacktriangledown\text{---}$), and 30°C ($\text{---}\circ\text{---}$), and allowed to further incubate for the indicated times. Results represent the mean \pm SEM for $n = 4$ determinations. Total uptake values (3.68 ± 0.18 nmol/mg protein) were determined after the 5 min incubation with $^3\text{H-L-glutamate}$, but prior to dilution.

Figure 5.5 Stimulatory effect of exogenous L-glutamate on the efflux of ^3H -L-glutamate from synaptic vesicles.



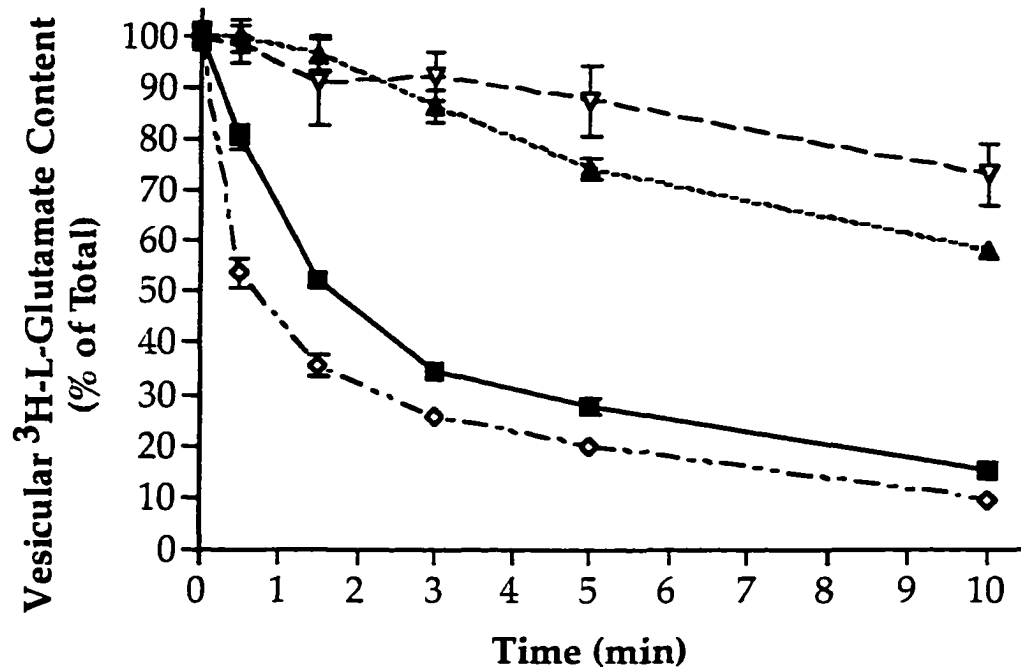
The uptake of ^3H -L-glutamate was performed as described in Chapter 2. Following a 5 min incubation, assays were diluted 20 fold into buffers including ($--\Delta--$) or devoid of 20 mM L-glutamate ($—\blacksquare—$), and then terminated at the indicated times. Results represent the mean \pm SEM for $n = 3$ determinations. Total uptake values (3.46 ± 0.21 nmol/mg protein) were determined after the 5 min incubation with ^3H -L-glutamate, but prior to dilution. Statistical analyses were performed using the Students T test with alternate Welch's test correction yielding values of $p < 0.05$ (*) where indicated.

the transporter binding site (assured by testing a compound at 10x its K_i value), an excellent substrate would exchange rapidly, evidenced by increasing efflux, while a poor substrate would exchange more slowly and decrease the rate of efflux. Carried to an extreme, a non-substrate inhibitor should essentially block efflux altogether. This latter effect was observed with Congo Red (Figure 5.6). When synaptic vesicles containing accumulated ^3H -L-glutamate were diluted 20 fold into buffer containing 2 μM Congo Red, the amount of efflux was reduced to about the level previously observed at 0°C . Further, the inclusion of an excess of Congo Red (20 μM , 40x its K_i) relative to L-glutamate (20 mM, 10x its K_i) inhibited the *trans*-stimulation. These results are consistent with both the binding of Congo Red to the substrate site and the inability of Congo Red to be translocated into the vesicle (e.g. a non-substrate inhibitor).

Inhibitor dependent attenuation of vesicular ^3H -L-glutamate efflux

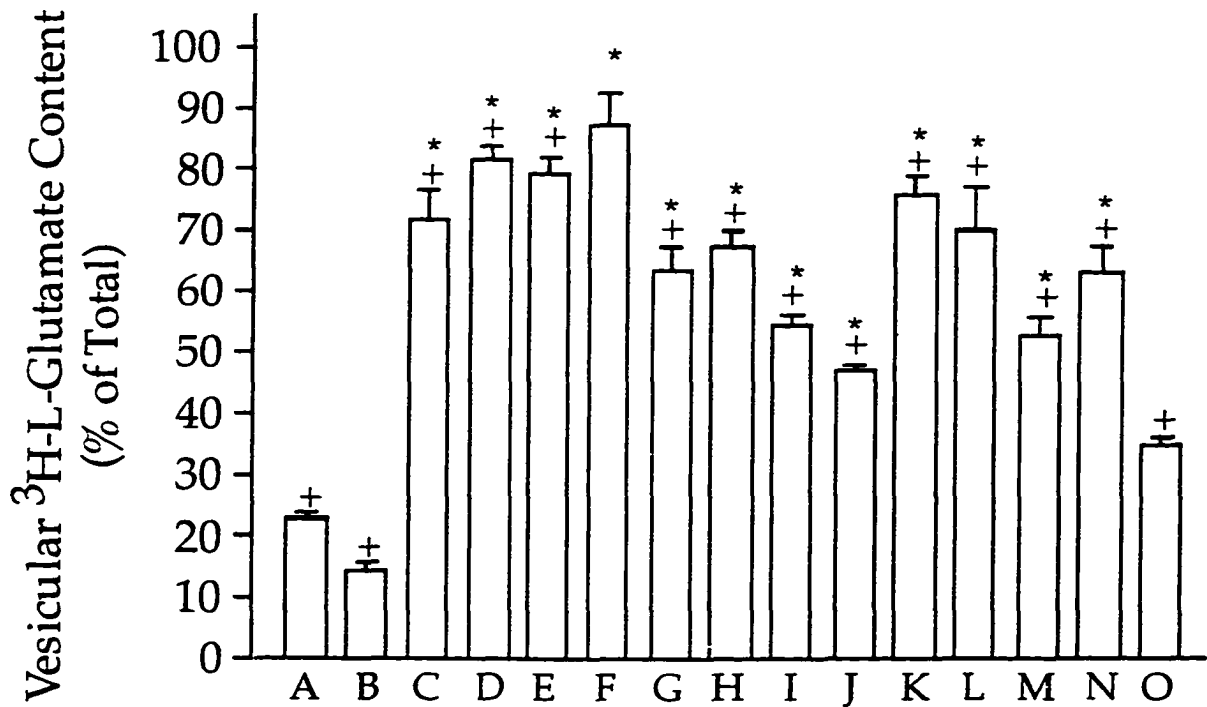
As illustrated in Figure 5.7, the inclusion of various uptake inhibitors identified in Chapters 3 and 4 produced a range of effects on the rate of vesicular ^3H -L-glutamate efflux, when included in the dilution buffers at 10x their K_i values. As expected, the presence of 20 mM L-glutamate in the dilution buffer produced a slight increase in the efflux rate. This

Figure 5.6 Inhibitory effect of Congo Red on the efflux of ^3H -L-glutamate from synaptic vesicles



The uptake of ^3H -L-glutamate was performed as described in Chapter 2. Assays were diluted 20 fold into buffers including; 20 μM Congo Red and 20 mM L-glutamate (— ∇ —), 2 μM Congo Red (— \blacktriangle —), Control (— \blacksquare —), 20 mM L-glutamate (— \diamond —), and terminated at the indicated times. Results represent the mean \pm SEM for $n = 6$ determinations. Total uptake values (2.86 ± 0.30 nmol/mg protein) were determined after the 5 min incubation with ^3H -L-glutamate, but prior to dilution.

Figure 5.7 Inhibitory effects of vesicular glutamate transport inhibitors on the efflux of $^3\text{H-L-glutamate}$ from synaptic vesicles.



The uptake of $^3\text{H-L-glutamate}$ from synaptic vesicles was performed as described in Chapter 2. Assays were diluted 20 fold into buffers including: Control (A), 20 mM L-glutamate (B), 2 μM Chicago Sky Blue (C), 2 μM Evans Blue (D), 3 μM Naphthol Blue Black (E), 5 μM Congo Red (F), 40 μM Gallion (G), 50 μM Chromotrope 2R (H), 60 μM Nitro Red (I), 300 μM Azophloxine (J), 10 mM Chicago Acid (K), 20 mM 4-amino-5-hydroxy-1-naphthalene sulfonic acid (L), 2 mM xanthurenic acid (M), 10 mM kynurenic acid (N), 4 mM (\pm) *trans*-ACPD (O), and terminated after a 5 min incubation. Results represent the mean \pm SEM for $n = 6-8$ determinations. Total uptake values (2.96 ± 0.16 nmol/mg protein) were determined after the 5 min preloading with $^3\text{H-L-glutamate}$, but prior to dilution. Statistical analyses were performed using a one-way ANOVA test followed by the Tukey's multiple comparison test and represent $p < 0.05$ for differences from total uptake (+) and control (*) values.

enhancement would have been larger (and statistically significant) if the assays had been terminated earlier (see Figure 5.5). Not surprisingly, the majority of the disulfonic acid dyes, including Congo Red, Chicago Sky Blue, and Evans Blue, proved to be either very poor or non-substrates. However, a few of the compounds (e.g. Nitro red, Azophloxine, xanthurenic acid, and kynurenic acid) were able to exchange with the intra-vesicular $^3\text{H-L}$ -glutamate, albeit at about half of the rate at which L-glutamate exchanged. These results are quite interesting, as they suggest that in some instances, certain naphthalene sulfonic acid dyes and kynurenic acid analogues can actually serve as substrates of the transporter. As a positive control, (\pm) *trans*-ACPD, which had previously been shown to be a vesicular transporter substrate (Winter and Ueda, 1993), was also included in the assay. It slowed but did not completely block the efflux of $^3\text{H-L}$ -glutamate, as would be expected of a moderate substrate.

Discussion

The results of this study help to shed new light on the mechanism of the vesicular glutamate transporter. The evidence suggests that vesicular glutamate transport is dependent upon both proton and substrate concentration gradients, and occurs via a distinct bi-directional carrier-

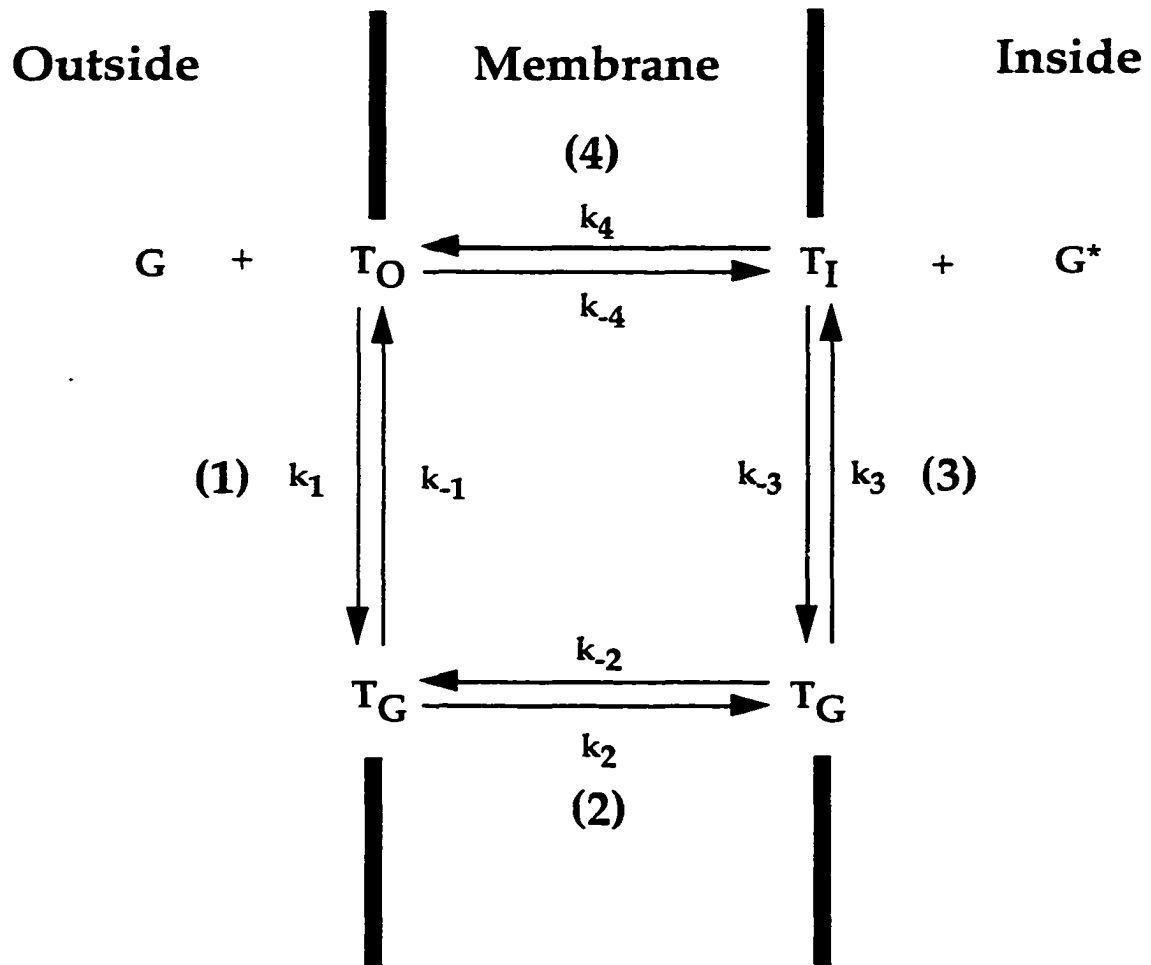
mediated transport process. Previous studies have characterized the requirement of ATP in the uptake of L-glutamate into synaptic vesicles (Naito and Ueda, 1983; Naito and Ueda, 1985). Here, it is demonstrated that under the experimental conditions employed, ATP is also necessary to maintain accumulated levels of glutamate within the vesicles once it is sequestered (Figures 5.1 and 5.2). This finding is particularly interesting in view of the various disorders in which CNS ATP levels are depleted (e.g. ischemia, hypoxia, and hypoglycemia) (for review see Choi (1990). Since synaptic vesicles represent a significant pool of glutamate in EAA neuronal terminals, liberation of this glutamate reserve into cellular compartments could potentially impact the degree of neurotoxicity incurred during periods of damage.

The extent to which glutamate is concentrated in synaptic vesicles is also affected by its concentration gradient across the vesicular membrane. This is depicted in Figures 5.4 - 5.6 when, following a 20 fold dilution of vesicles containing accumulated ^3H -L-glutamate into buffer devoid of glutamate and ATP, a rapid efflux occurred. Previous investigations revealed that under similar experimental conditions, the proton gradient was maintained, even during glutamate efflux (Carlson and Ueda, 1990; Wang and Floor, 1994). This would suggest that the efflux is primarily due to a decrease in the glutamate concentration gradient, rather than a loss in the driving force for uptake. Therefore, under normal uptake conditions, efflux

may be occurring simultaneously, albeit at a lower rate. This implies that the glutamate pool in synaptic vesicles, may turn over as a function of time, as opposed to remaining static once quantal levels are reached. Under normal physiological conditions, however, this would be difficult to observe considering that net transport is into the vesicles, and since sufficient cytosolic glutamate levels exist to replenish those lost from the vesicular pool from a relatively moderate level of efflux.

The observation that the efflux rate of accumulated vesicular glutamate is enhanced in the presence of external substrate (Figures 5.5 and 5.6), supports the hypothesis that this efflux is occurring via a bi-directional carrier-mediated process and is consistent with the concept of *trans*-stimulation. Such relationships are more easily visualized using a simple model of the transport mechanism. As illustrated in Figure 5.8, there are two stages which comprise carrier-mediated transport. The first involves the binding, translocation, and release of substrate across the membrane, and the second entails resetting this transport mechanism to its original orientation. As the evidence suggests that vesicular glutamate transport is bi-directional, these processes may occur in either direction. In order for *trans*-stimulation to occur, migration of the unoccupied site (Figure 5.8, step (4) k_4/k_{-4}) must be slow relative to the migration of the occupied transporter site (step (2) k_2/k_{-2}). As shown in Figure 5.5, efflux can occur in the absence of external substrate, and suggests that the unoccupied vesicular glutamate transporter is able to

Figure 5.8 Model of glutamate induced *trans*-stimulation for the vesicular transport system.



G - unlabeled L-glutamate

G^* - ^3H -L-glutamate

T_o - unoccupied transporter site on extra-vesicular surface

T_i - unoccupied transporter site on intra-vesicular surface

migrate across the membrane (step (4) k_{-4}). If this were not so, efflux would be limited to the transport of only one glutamate molecule per transporter since the mechanism would be unable to reset. In the presence of a saturating concentration of external substrate (20 mM L-glutamate), the rate of efflux is accelerated since the transporter returning to the intravesicular surface is now occupied (step (2) k_2), allowing for a faster migration and therefore a higher availability of the transporter site on the intravesicular surface (T_i). Moreover, while sufficiently high concentrations of substrate exist on either side of the membrane, migration of the unoccupied transporter (k_4/k_{-4}) will be reduced, and the transport mechanism will cycle between steps k_1, k_2, k_3 and k_{-3}, k_{-2}, k_{-1} thereby accelerating the efflux rate. This is the paradigm observed in the instance of *trans*-stimulation.

One final reference should be made to this mechanism regarding the process occurring during the normal net uptake of glutamate. It has been proposed that glutamate is concentrated in synaptic vesicles up to a level 10 times higher than that in the cytosol (Maycox et al., 1990). For this to take place, transport into synaptic vesicles must occur at a higher level than the rate of efflux (i.e. $k_2 > k_{-2}$). While presently there is a lack of sufficient evidence to rationalize this occurrence, it is likely due to either differences in the concentration gradients of the requisite transport ions (e.g. H^+ and Cl^-) across the vesicular membrane, and/or differences in the substrate affinities on the extra- and intravesicular surfaces of the transport protein

(i.e. $K_m \text{ outside} > K_m \text{ inside}$).

In contrast to the demonstration of *trans*-stimulation in this study, it was previously reported by Wang and Floor (1994) that the rate of vesicular $^3\text{H-L-glutamate}$ efflux is not stimulated by the application of external substrate. This lack of efflux stimulation, however, may be explained by the low concentration of L-glutamate (500 μM) that was included in the dilution buffer of their experiments. Since this concentration is 2-6 fold lower than the K_m value (1-3 mM) of the vesicular glutamate transporter, saturation of the substrate binding site would not be obtained and competition for the migration of the unoccupied vs. occupied transporter site would exist (k_4 vs. k_2 , Figure 5.8). Indeed, in the present study, 20 mM L-glutamate ($10 \times K_m$) was included in the dilution buffer to insure saturation of the substrate site, and obtain a significant level of efflux stimulation (Figure 5.5).

Three criteria have been met by Congo Red in these experiments which identify it as a nontransportable inhibitor of vesicular glutamate uptake. First, the nature of its inhibition is competitive (Figure 4.2). Second, it does not exchange with accumulated vesicular $^3\text{H-L-glutamate}$ (Figure 5.6). Third, it can attenuate the glutamate induced *trans*-stimulation (Figure 5.6). Referring to Figure 5.8, its action is likely to bind to the unoccupied transporter site on the extravesicular surface (T_o), and effectively "lock" it in this position by a saturated level of binding. Whereas a substrate such as L-glutamate may bind and accelerate the migration rate of the occupied

transporter across the membrane, a non-transportable inhibitor will completely prevent its movement. This activity is evidenced when Congo Red was included in the dilution buffer and the resulting efflux rate was lower than that of the Control.

Since the chemical configuration of the vesicular glutamate transporter protein is yet unknown, the optimal binding requirements for substrates and non-substrates is also not known. It is likely, though, that the inability of Congo Red to be transported is at least partly due to its large rigid and bulky structure which may interfere with the proper conformational folding of the transporter protein. Conversely, there must exist certain intrinsic chemical qualities of the smaller more flexible compound L-glutamate which allows it to bind and be translocated. Fortunately, the ability of these compounds to either stimulate or block the efflux of accumulated $^3\text{H-L-glutamate}$ from synaptic vesicles allows for their categorization as transportable or non-transportable inhibitors. In the experiments summarized in Figure 5.7, several of the vesicular uptake inhibitors identified previously were tested in this manner. Although many of these compounds completely or nearly completely blocked the efflux of $^3\text{H-L-glutamate}$, a few, including Nitro red, Azophloxine, xanthurenic acid and (\pm)trans-ACPD only partially inhibited efflux. This suggests that these compounds were able to exchange with the accumulated $^3\text{H-L-glutamate}$, admittedly at a much slower rate than the endogenous substrate L-glutamate. It is therefore possible to conclude that

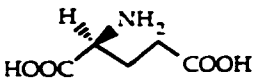
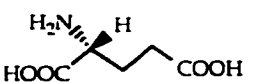
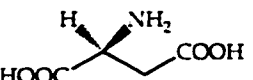
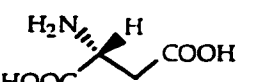
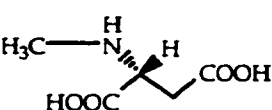
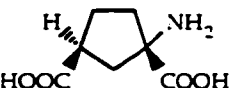
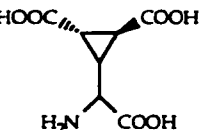
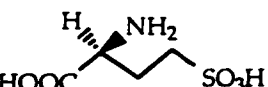
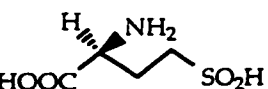
these compounds act as partial substrates of the vesicular glutamate transporter.

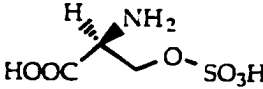
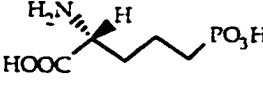
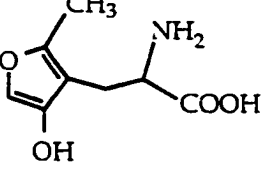
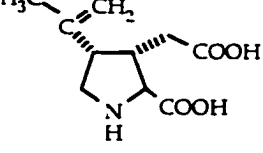
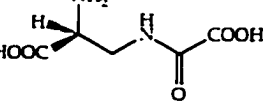
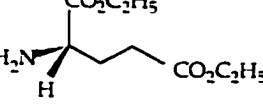
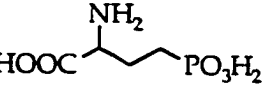
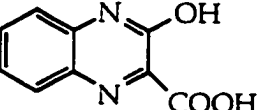
Given the small size of this sample set of compounds, it is yet too early to draw any conclusions regarding the chemical characteristics which differentiate transportable from non-transportable inhibitors. Further work must be directed towards expanding these groups in order to begin to discern differences between them. The rapidity of this technique as a means of differentiating potential substrates from non-substrates may aid in the eventual compilation of their respective pharmacophores.

Chapter 6: Cross-reactivities of EAA analogues with the vesicular glutamate transporter

Initial studies examined the inhibitory properties of several EAA analogues on the uptake of ^3H -L-glutamate (0.25 mM) into synaptic vesicles. This series of experiments was undertaken to identify lead inhibitors of vesicular glutamate uptake and address their potential cross-specificities with other components of the EAA system. When included in the assays at a final concentration of 5 mM, a range of activity for these compounds was observed (Table 6.1), although few reduced uptake more than the endogenous substrate L-glutamate (28.9 % of Control). Two exceptions to these findings were (\pm) *trans*-ACPD (11.7 % of Control) (see Chapter 3) and L-*anti-endo*-MPDC (20.5 % of Control). The latter being a potent transportable inhibitor of the high-affinity Na^+ -dependent EAA transporter (Bridges et al., 1994). The lack of cross-reactivity observed with many of these EAA analogues suggests that the vesicular glutamate transporter is pharmacologically distinct, and encourages the search for more potent selective inhibitors of this system.

Table 6.1 Cross-reactivities of EAA analogues with the vesicular glutamate transporter

Compound	Structure	Vesicular Uptake of ^3H -L-Glutamate (% of Control)	EAA Activity
L-Glutamic acid		28.9 ± 1.4 (8)	Endogenous broad spectrum EAA agonist
D-Glutamic acid		63.0 ± 1.8 (3)	NMDA agonist
L-Aspartic acid		$79.0 \pm 8.7^*$ (2)	NMDA agonist
D-Aspartic acid		95.9 ± 1.1 (4)	NMDA agonist
NMDA		$96.9 \pm 4.4^*$ (2)	NMDA agonist
<i>cis</i> -ACPD		87.2 ± 6.1 (3)	NMDA agonist
DCG-IV		100 (1)	NMDA agonist, Group II mGluR agonist
L-Homocysteic acid		92.2 ± 2.7 (3)	NMDA agonist
L-Homocysteine sulphinic acid		$84.9 \pm 1.5^*$ (2)	NMDA agonist

Compound	Structure	Vesicular Uptake of ^3H -L-Glutamate (% of Control)	EAA Activity
L-Serine-O-sulphate		$91.8 \pm 6.9^*$ (2)	NMDA agonist
D-AP5		$92.1 \pm 3.6^*$ (2)	NMDA antagonist
AMPA		$87.0 \pm 0.4^*$ (2)	AMPA agonist
KA		$92.1 \pm 3.6^*$ (2)	KA agonist
β -L-ODAP		100 (1)	AMPA/KA agonist
L-Glutamic acid diethyl ester		100 (1)	Noncompetitive AMPA antagonist
D,L-AP4		89.0 ± 5.1 (3)	Non-selective inotropic EAA antagonist; Group III mGluR agonist
3-Hydroxy-2-quinoxaline carboxylic acid		69.5 ± 2.3 (5)	Non-selective inotropic EAA antagonist

Compound	Structure	Vesicular Uptake of ^3H -L-Glutamate (% of Control)	EAA Activity
L- α -AA		$89.8 \pm 9.5^*$ (2)	Non-selective inotropic EAA antagonist
(\pm) <i>trans</i> -ACPD		11.7 ± 1.2 (5)	Group I and II mGluR agonist
(R,S) 3-Hydroxyphenylglycine		$100 \pm 0^*$ (2)	Group I mGluR agonist
D,L-AP3		87.0 ± 5.8 (3)	Group I mGluR antagonist
L-Aspartate- β -hydroxamate		100 (1)	Group I mGluR antagonist
L- <i>anti</i> -endo-MPDC		20.5 ± 0.8 (5)	EAA cellular reuptake inhibitor
L- <i>trans</i> -2,4-PDC		71.7 ± 2.1 (5)	EAA cellular reuptake inhibitor
L- <i>anti</i> -exo-MPDC		$85.7 \pm 0.4^*$ (2)	EAA cellular reuptake inhibitor

Compound	Structure	Vesicular Uptake of $^3\text{H-L-Glutamate}$ (% of Control)	EAA Activity
L-Cysteic acid		85.5 (1)	EAA cellular reuptake inhibitor
D-Cysteic acid		93.3 (1)	EAA cellular reuptake inhibitor
meso-MPDC		100 (2)	EAA cellular reuptake inhibitor
D,L-threo- β -Hydroxyaspartic acid		100 (1)	EAA cellular reuptake inhibitor
L-DHK		89.0 \pm 4.8 (3)	EAA cellular reuptake inhibitor

The uptake of $^3\text{H-L-glutamate}$ (0.25 mM) into synaptic vesicles was performed as described in Chapter 2. EAA analogues were present in the incubation medium at a final concentration of 5 mM. Results are reported as a percentage of Control uptake \pm SEM or SD* with n number of experiments in parentheses. Abbreviations: NMDA, N-Methyl-D-aspartic acid; (\pm) *cis*-ACPD, (\pm)-1-Aminocyclopentane-*cis*-1,3-dicarboxylic acid; DCG IV, (2S,2'R,3'R)-2-(2',3'-Dicarboxycyclopropyl)glycine; D-AP5, D(-)-2-Amino-5-phosphonopentanoic acid; AMPA, (R,S)- α -Amino-3-hydroxy-5-methyl-4-isoxazolepropionic acid; KA, Kainic acid; β -L-ODAP, β -N-Oxalyl-L- α,β -diaminopropionic acid; D,L-AP4, D,L-2-Amino-4-phosphonobutyric acid; L- α -AA, L- α -Amino adipic acid; (\pm) *trans*-ACPD, (\pm)-1-Aminocyclopentane-*trans*-1,3-dicarboxylic acid; ; D,L-AP3, D,L-2-Amino-3-phosphonobutyric acid;

L-anti-endo-MPDC, *L-anti-endo-3,4-Methanopyrrolidinedicarboxylic acid*; *L-trans-2,4-PDC*, *L-trans -2,4-Pyrrolidinedicarboxylic acid*; *L-anti-exo-MPDC*, *L-anti-exo-3,4-Methanopyrrolidinedicarboxylic acid*; *meso-MPDC*, *meso-3,4-Methanopyrrolidinedicarboxylic*; *L-DHK*, *L-Dihydrokainic acid*.

Chapter 7: Conclusions and future directions

Within the last 30 years, our knowledge and understanding of the EAA neurotransmitter system has increased dramatically. Numerous advances have been made towards the pharmacological and molecular characterization of many of its components (e.g. ionotropic and metabotropic receptors, cellular transporters, enzymatic processes). In spite of this progress, one key area of EAA research has lagged behind, namely, the characterization of the transporter responsible for packaging glutamate into synaptic vesicles. In part, this is due to the lack of potent and selective inhibitors of this transport process. With this in mind, the work in this study was specifically focused on further resolving this issue.

Two series of inhibitors in particular have been studied in depth to aid in the formulation of a vesicular glutamate pharmacophore. The first is based upon a rigid bicyclic quinoline core framework and includes kynurenate, 7-Cl-kynurenate, and xanthurenate. The second is based upon a bicyclic naphthalene framework, but incorporates one or two diazo-linked aromatic substituents, as seen in the structures of the dyes Evans Blue, Chicago Sky Blue, Congo Red, and Naphthol Blue Black. Taken together, a number of conclusions can be drawn about the structure-activity

relationships of these compounds with the vesicular glutamate transporter by examining their inhibitory activities.

- **A substituted bicyclic ring framework (e.g. quinoline or naphthalene) can potentially mimic the conformation of glutamate which binds to the vesicular transporter.** The determination that many of these compounds were competitive inhibitors suggested that something intrinsic about their structures resembled the conformation of L-glutamate which binds to the vesicular transporter. Therefore a model has been proposed for the quinoline analogues in which the carbocyclic ring mimics the γ -carboxylate of L-glutamate (Figures 3.2 and 3.3). This is supported by the finding that electron donating groups attached to positions 7 or 8 as in 7-Cl-kynurenate and xanthurenate, markedly increase inhibitory activity. Presumably, this is due to the increased electron density of the carbocyclic ring which may more closely approximate the carboxylate of glutamate. Further, analogous compounds lacking the carbocyclic ring are poor inhibitors (Table 3.1).
- **Inhibitory potency is dramatically increased with the attachment of diazo-linked aromatic side chains.** This is supported by the finding that compounds incorporating these diazo-linked side chains exhibit increased inhibitory activity over the analogous naphthalene sulfonic acids which

lack them (Chapter 4). Since this is clearly a structural feature not associated with the endogenous substrate L-glutamate, it is likely that the mode in which these competitive inhibitors bind to the transporter is different. For instance, the aromatic side chain may be appropriately positioned to interact with a lipophilic moiety of the protein in the binding pocket. Moreover, the significantly increased affinity of these compounds compared to that of L-glutamate (up to 10,000 fold) suggests that closely mimicking a glutamate conformer may not be optimal for inhibitory activity.

Following the identification of the inhibitory properties of these compounds, further investigations into the mechanism of vesicular glutamate transport were conducted. Using these inhibitors as probes, several important findings were made.

- **Efflux of accumulated vesicular ^3H -L-glutamate can be stimulated by exogenous concentrations of substrate.** This is the first clear demonstration of glutamate induced *trans*-stimulation reported for the vesicular system (Chapter 5). It suggests that vesicular glutamate transport is not only carrier-mediated, but also bi-directional. Further, these findings suggest that the *in vivo* pool of vesicular glutamate may turn

over as a function of time due to a continuous homo-exchange between extra- and intravesicular pools.

- **Vesicular ^3H -L-glutamate efflux can be blocked by an exogenous nontransportable inhibitor.** In contrast to the substrate-induced stimulation of efflux, these findings indicate that certain competitive uptake inhibitors can attenuate the efflux of the vesicular neurotransmitter contents. This observation is particularly interesting, since in comparison to the activity of a substrate, it allows for the differentiation of transportable from non-transportable inhibitors, based upon their abilities to either stimulate or attenuate the efflux of ^3H -L-glutamate from synaptic vesicles (Figure 5.7).

Presented within this study, both the inhibitor pharmacology and insight into the transport mechanism further the progress towards the eventual characterization of this important transport system. Still, there is a great need for additional work to address several key issues. For example, while an important inhibitory role has been demonstrated for the diazo-linked aromatic side chain of the naphthylamine sulfonic acid dyes, additional studies should attempt to elucidate its binding interaction. Are there limitations on the regio-positioning of this group around the naphthalene ring, or restrictions on the length of the aromatic chain? Is the

diazo-group even required within this linkage? Additionally, there is a great deal of flexibility in the positioning of ionic functional groups around the quinoline and naphthalene ring systems of these compounds. Therefore, studies should address their contribution to transport inhibition.

In addition to inhibitory potency at the vesicular transporter, future studies should be directed towards the development of compounds exhibiting little cross-reactivity with other sites of EAA activity. A few of the compounds identified in this study (e.g. xanthurenate, Nitro Red, Azophloxine, and Chromotrope 2R) fall into this category and may prove to be useful templates for the development of even more potent analogues. The utility of such selective inhibitors would be manifold. Their selective affinity could be exploited for the isolation and molecular characterization of the vesicular transport protein. Additionally, they could serve as useful pharmacological probes and modulators of glutamatergic processes *in vivo*.

Along with the increasing evidence that the EAA system participates in a wide range of cognitive functions, comes its untapped potential for pharmacological manipulation. In certain CNS pathologies, a failure to regulate extracellular glutamate concentrations has contributed to excitotoxic-mediated neuronal injury. Presently, EAA ionotropic receptor antagonists are under investigation as possible drug candidates. As an alternative, regulation of presynaptic glutamate pools prior to release may prove to be

beneficial in these disorders. In this vein, inhibitors of vesicular glutamate uptake may show promise.

Clearly, vesicular glutamate transport is an essential and yet poorly understood component of the glutamatergic system. Progress into the characterization of the transporter pharmacophore will not only further our understanding of this system but provide tools with which to explore its function.

References:

- Arriza, J. L., Fairman W. A., Wadiche J. I., Murdoch G. H., Kavanaugh M. P. and Amara S. G. (1994) Functional comparisons of three glutamate transporter subtypes cloned from human motor cortex. *J. Neurosci.* **14**(9): 5559-5569.
- Booth, R. F. G. and Clark J. B. (1978) A rapid method for the preparation of relatively pure metabolically competent synaptosomes from rat brain. *Biochem. J.* **176**: 365-370.
- Bridges, R. J., Lovering F. E., Koch H., Cotman C. W. and Chamberlin A. R. (1994) A conformationally constrained competitive inhibitor of the sodium-dependent glutamate transporter in forebrain synaptosomes: L-anti-endo-3,4-methanopyrrolidine dicarboxylate. *Neurosci. Lett.* **174**: 193-197.
- Bridges, R. J., Stevens D. R., Kahle J. S., Nunn P. B., Kadri M. and Cotman C. W. (1989) Structure-function studies on N-oxalyl-diamino-dicarboxylic acids and excitatory amino acid receptors: evidence that β -L-ODAP is a selective non-NMDA agonist. *J. Neurosci.* **9**(6): 2073-2079.
- Burger, P. M., Mehl E., Cameron P. L., Maycox P. R., Baumert M., Lottspeich F., Camilli P. D. and Jahn R. (1989) Synaptic vesicles immunisolated from rat cerebral cortex contain high levels of glutamate. *Neuron* **3**: 715-720.
- Carlson, M. D., Kish P. E. and Ueda T. (1989) Glutamate uptake into synaptic vesicles: competitive inhibition by bromocriptine. *J. Neurochem.* **53**(6): 1889 - 1894.
- Carlson, M. D. and Ueda T. (1990) Accumulated glutamate levels in the synaptic vesicle are not maintained in the absence of active transport. *Neurosci. Lett.* **110**: 325 - 330.
- Chamberlin, A. R., Koch H. P. and Bridges R. J. (1998) Design and synthesis of conformationally constrained inhibitors of the high-affinity, sodium-dependent glutamate transporters. *Methods Enzymol.* **296**: 175-189.
- Chamberlin, R. and Bridges R. (1993) Conformationally constrained acidic amino acids as probes of glutamate receptors and transporters. Drug design for neuroscience. New York, Raven Press. 231-259.

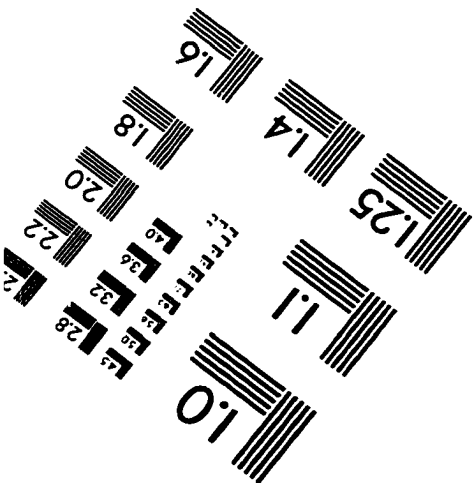
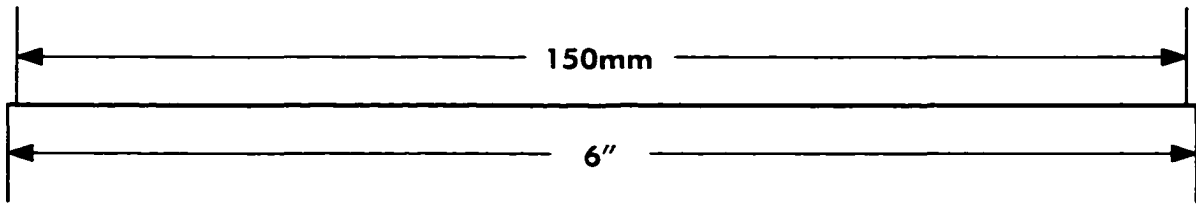
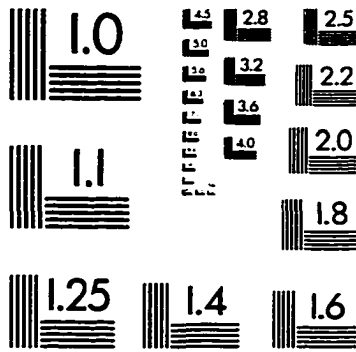
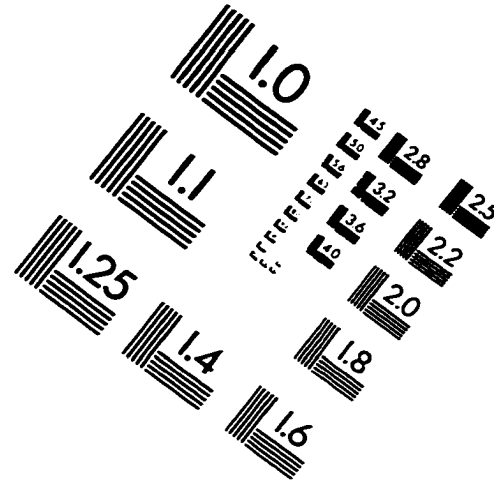
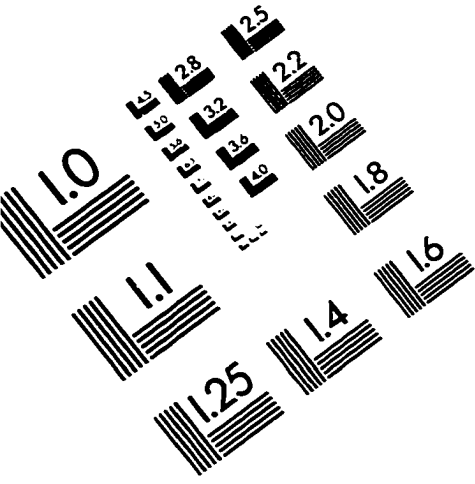
- Cheng, Y.-C. and Prusoff W. H. (1973) Relationship between the inhibition constant (K_i) and the concentration of inhibitor which causes 50 percent inhibition (I_{50}) of an enzymatic reaction. *Biochem. Pharmacol.* **22**: 3099-3108.
- Choi, D. W. (1990) The role of glutamate neurotoxicity in hypoxic-ischemic neuronal death. *Annu. Rev. Neurosci.* **13**: 171-182.
- Christensen, H. N. (1975) Biological transport. Reading, MA, W.A. Benjamin, Inc.
- Clark-Lewis, J. W. and Mortimer a. P. I. (1961) The 4-hydroxypipericolic acid from *Acacia* species and its stereoisomers. *J. Chem. Soc.* : 189-201.
- Conn, P. J. and Pin J. P. (1997) Pharmacology and functions of metabotropic glutamate receptors. *Annu. Rev. Pharmacol. Toxicol.* **37**: 205-237.
- Cotman, C. W., Kahle J. S., Miller S. E., Ulas J. and Bridges R. J. (1995) Excitatory amino acid neurotransmission. Psychopharmacology: The fourth generation of progress. New York, Raven. 75-85.
- De Belleruche, J. S. and Bradford H. F. (1973) Amino acids in synaptic vesicles from mammalian cerebral cortex: A reappraisal. *J. Neurochem.* **21**: 441 - 451.
- De Belleruche, J. S. and Bradford H. F. (1977) On the site of origin of transmitter amino acids released by depolarization of nerve terminals *in vitro*. *J. Neurochem.* **29**: 335-343.
- Floor, E., Leventhal P. S., Wang Y., Mang L. and Chen W. (1995) Dynamic storage of dopamine in rat brain synaptic vesicles *in vitro*. *J. Neurochem.* **64**(2): 689-699.
- Fyske, E. M., Iversen E. G. and Fonnum F. (1992) Inhibition of L-glutamate uptake into synaptic vesicles. *Neurosci. Lett.* **135**: 125 - 128.
- Ganong, A. H., Lanthorn T. H. and Cotman C. W. (1983) Kynurenic acid inhibits synaptic and acidic amino acid-induced responses in the rat hippocampus and spinal cord. *Brain Res.* **273**: 170-174.
- Garlin, A., Sinor A., Lee S., Grinspan J. and Robinson M. (1995) Pharmacology of sodium-dependent high affinity L-[3 H]glutamate transport in glial cultures. *J. Neurochem.* **64**: 2572-2580.

- Gegelashvili, G. and Schousboe A. (1997) High affinity glutamate transporters: Regulation of expression and activity. *Mol. Pharmacol.* 52: 6-15.
- Ham, N. S. (1974) NMR studies of solution conformations of physiologically active amino acids. Molecular and quantum pharmacology. Dordrecht, Holland, D. Reidel Pub. Co. 261-286.
- Harteringer, J. and Jahn R. (1993) An anion binding site that regulates the glutamate transporter of synaptic vesicles. *J. Bio. Chem.* 268(31): 23122 - 23127.
- Honore, T., Lauridsen J. and Krogsgaard-Larsen P. (1982) The binding of [³H]AMPA, a structural analogue of glutamic acid to rat brain membranes. *J. Neurochem.* 38(1): 173-178.
- Keller, B. U., Blaschke M., Rivosecchi R., Hollmann M., Heinemann S. F. and Konnerth A. (1993) Identification of a subunit-specific antagonist of α -amino-3-hydroxy-5-methyl-4-isoxazolepropionate/kainate receptor channels. *Neurobio.* 90: 605-609.
- Kessler, M., Terramani T., Lynch G. and Baudry M. (1989) A glycine site associated with N-methyl-D-aspartic acid receptors: Characterization and identification of a new class of antagonists. *J. Neurochem.* 52: 1319-1328.
- Kish, P. E. and Ueda T. (1989) Glutamate accumulation into synaptic vesicles. *Methods Enzymol.* 174: 9-25.
- Kuhar, M. J. and Zarbin M. A. (1978) Synaptosomal transport: A chloride dependence for choline, GABA, glycine and several other compounds. *J. Neurochem.* 31: 251-256.
- London, E. D. and Coyle J. T. (1979) Specific binding of ³H-kainic acid receptor site in rat brain. *Mol. Pharmacol.* 15: 492-505.
- Maycox, P. R., Deckwerth T., Hell J. W. and Jahn R. (1988) Glutamate uptake by brain synaptic vesicles: Energy dependence of transport and functional reconstitution in proteoliposomes. *J. Biol. Chem.* 263(30): 15423 - 15428.
- Maycox, P. R., Hell J. W. and Jahn R. (1990) Amino acid neurotransmission: Spotlight on synaptic vesicles. *TINS* 13(3): 83 - 87.

- McMahon, H. T. (1991) The bioenergetics of neurotransmitter release. *Biochim. Biophys. Acta.* 1059: 243-264.
- Monaghan, D. T. and Cotman C. W. (1986) Identification and properties of N-methyl-D-aspartate receptors in rat brain synaptic plasma membranes. *Proc. Natl. Acad. Sci.* 83(19): 7532-7536.
- Naito, S. and Ueda T. (1983) Adenosine triphosphate-dependent uptake of glutamate into protein I-associated synaptic vesicles. *J. Biol. Chem.* 258(2): 696 - 699.
- Naito, S. and Ueda T. (1985) Characterization of glutamate uptake into synaptic vesicles. *J. Neurochem.* 44(1): 99 - 109.
- Nicholls, D. G. and Sihra T. S. (1986) Synaptosomes possess an exocytotic pool of glutamate. *Nature* 321: 772-773.
- Ozkan, E. D., Lee F. S. and Ueda T. (1997) A protein factor that inhibits ATP-dependent glutamate and γ -aminobutyric acid accumulation into synaptic vesicles: Purification and initial characterization. *Proc. Natl. Acad. Sci.* 94: 4137-4142.
- Ozkan, E. D. and Ueda T. (1998) Glutamate transport and storage in synaptic vesicles. *Jpn. J. Pharmacol.* 77(1): 1-10.
- Price, C. J. and Raymond L. A. (1996) Evans Blue antagonizes both α -amino-3-hydroxy-5-methyl-4-isoxazolepropionate and kainate receptors and modulates receptor desensitization. *Mol. Pharmacol.* 50: 1665-1671.
- Robinson, M. B., Schulte M. K., Freund R. K., Johnson R. L. and Koerner J. F. (1985) Structure-function relationships for kynurenic acid analogues at excitatory pathways in the rat hippocampal slice. *Brain Res.* 361: 19-24.
- Roseth, S., Fykse E. M. and Fonnum F. (1995) Uptake of L-glutamate into rat brain synaptic vesicles: Effect of inhibitors that bind specifically to the glutamate transporter. *J. Neurochem.* 65(1): 96 - 103.
- Roseth, S., Fyske E. M. and Fonnum F. (1998) Uptake of L-glutamate into synaptic vesicles: Competitive inhibition by dyes with biphenyl and amino- and sulphonic acid-substituted naphthyl groups. *Biochem. Pharmacol.* 56: 1243-1249.

- Shioi, J. and Ueda T. (1990) Artificially imposed electrical potentials drive L-glutamate uptake into synaptic vesicles of bovine cerebral cortex. *Biochem. J.* **267**: 63 - 68.
- Simon, J. R., Contrera J. F. and Kuhar M. J. (1976) Binding of [³H]kainic acid, an analogue of L-glutamate, to brain membranes. *J. Neurochem.* **26**: 141-147.
- Smith, P. K., Krohn R. I., Hermanson G. T., Mallia A. K., Gartner F. H., Provenzano M. D., Fujimoto E. K., Goeke N. M., Olson B. J. and Klenk D. C. (1985) Measurement of protein using bicinchoninic acid. *Anal. Biochem.* **150**: 76-85.
- Stone, T. W. (1993) Neuropharmacology of quinolinic and kynurenic acids. *Pharmacol. Rev.* **45**(3): 309-379.
- Storm-Mathisen, J., Leknes A. K., Bore A. T., Vaaland J. L., Edminson P., Finn-Morgens S. H. and Ottersen O. P. (1983) First visualization of glutamate and GABA in neurones by immunocytochemistry. *Nature* **301**: 517-520.
- Tabb, J. S., Kish P. E., Dyke R. V. and Ueda T. (1992) Glutamate transport into synaptic vesicles: Roles of membrane potential, pH gradient, and intravesicular pH. *J. Biol. Chem.* **267**(22): 15412 - 15418.
- Wang, y. and Floor E. (1994) Dynamic storage of glutamate in rat brain synaptic vesicles. *Neurosci. Lett.* **180**: 175 - 178.
- Watson, G. B., Hood W. F., Monahan J. B. and Lanthorn T. H. (1988) Kynurenate antagonizes actions of N-methyl-D-aspartate through a glycine-sensitive receptor. *Neurosci. Res. Com.* **2**(3): 169-174.
- Winter, H. C. and Ueda T. (1993) Glutamate uptake system in the presynaptic vesicle: Glutamic acid analogs as inhibitors and alternate substrates. *Neurochem. Res.* **18**(1): 79-85.
- Wu, H.-Q., Baran H., Ungerstedt U. and Schwarcz R. (1992) Kynurenic acid in the quinolinate-lesioned rat hippocampus: Studies *in vitro* and *in vivo*. *Eur. J. Neurosci.* **4**: 1264-1270.

IMAGE EVALUATION TEST TARGET (QA-3)



APPLIED IMAGE, Inc
 1653 East Main Street
 Rochester, NY 14609 USA
 Phone: 716/482-0300
 Fax: 716/288-5989

© 1993, Applied Image, Inc., All Rights Reserved

